THE UNIVERSITY OF MICHIGAN

College of Engineering
Mechanical Engineering Department
Cavitation and Multiphase Flow Laboratory

Report No UMICH 012449-9-T

LIQUID FILM THICKNESS TESTS - WET STEAM TUNNEL

by

F. G. Hammitt
J. B. Hwang
A. Mancuso
D. Krause
S. Blome

Financial Support Provided by:

National Science Foundation
Grant No. 40130

June 1975

ABSTRACT

Measured liquid film thicknesses along a flat blade immersed in high-velocity (to Mach 1) low-pressure ($\sim$ 3 psia) wet steam flow (wetness $\sim$ 5%), wherein water is injected through a transverse slit near the blade leading edge, are compared with film thickness predictions based upon the interfacial shear between steam and liquid flows. Tests are made for both adiabatic and diabatic (cold water injection) conditions. Good qualitative agreement is achieved, but an absolute discrepancy ($\sim$ x 2) exists between measured and predicted film thicknesses.

Comparison with predicted film thickness and steam velocity conditions for film breakdown into axial filaments or other dry spots shows that such transition occurs only under much smaller film thickness and steam velocity conditions than have been previously predicted.

Wave frequency ($\sim$10 Hz) and relative surface wave heights have been measured for the liquid film. Wave propagation velocity can only be estimated when film photographs to allow estimation of wave length are available.

ACKNOWLEDGMENTS

Many past and present laboratory personnel, in addition to the authors, have assisted in the work contributing to this report. In particular, we would like to thank Dr. J. Mikielewicz and Messrs. G. Ernst, D. N. Linh, and J. Tully. Financial support was provided under NSF Grant No. GK-40130.

List of Tables

1. Thermodynamic Operating Conditions of Steam Tunnel

List of Figures

1. Blade Profiles No. 1 and 2 (#1 - Condensed; and #2 - Injected Film)

2. Blade Profile No. 3 (Film Recovery Blade)

3. Electrical Conductivity Gages

4. Generalized Characteristics for Electrical Conductivity Thickness Gages

5. Film and Droplet Photos - Injected Water Film (Blade Profile No. 2)

6. Film and Droplet Photos - Injected and Condensed Films (Blade Profiles No. 1

7. Predicted Adiabatic Film Thickness vs Steam Velocity; Various Liquid Film F Rate

8. Experimental Adiabatic Film Thickness vs Steam Velocity; Liquid Film Flow R 5 cm^3/min.

9. Experimental Adiabatic Film Thickness vs Steam Velocity; Liquid Film Flow R 10 cm^3/min.

10. Experimental Adiabatic Film Thickness vs Steam Velocity; Liquid Film Flow 20 cm^3/min.

11. Experimental Adiabatic Film Thickness vs Steam Velocity; Liquid Film Flow 30 cm^3/min.

12. Experimental Adiabatic Film Thickness vs Steam Velocity; Liquid Film Flow 40 cm^3/min.

13. Experimental Adiabatic Film Thickness vs Steam Velocity; Liquid Film Flow 50 cm^3/min.

14. Variation of Liquid Film Thickness with Axial Position, Steam Velocity = 200

15. Variation of Liquid Film Thickness with Axial Position, Steam Velocity = 252

16. Variation of Liquid Film Thickness with Axial Position, Steam Velocity = 505

17. Variation of Liquid Film Thickness with Axial Position, Steam Velocity = 840

18. Variation of Liquid Film Thickness with Axial Position, Steam Velocity = 1042 f/s

19. Variation of Liquid Film Thickness with Axial Position, Steam Velocity = 1288 f/s

20. Predicted Diabatic (Cold Water) Film Thickness vs Steam Velocity; Various Liquid Film Flow Rates

21. Experimental Diabatic (Cold Water) Film Thickness vs Steam Velocity; Various Liquid Film Flow Rates

22. Photo of Droplets on Blade #3 Surface Showing Wetting Angle, Θ

23. Critical Film Thickness vs Steam Velocity, Various Wetting Angles, Liquid Temperature = 130^{O}F (Adiabatic Tests)

24. Critical Film Thickness vs Steam Velocity, Various Wetting Angles, Liquid Temperature = 70^{O}F (Diabatic Tests)

25. Oscilloscope Pictures of Thickness Gage Output

26. Liquid Film Surface Wave; Frequency vs Steam Velocity

I. INTRODUCTION

The wet-steam flow research program at the University of Michigan has been described previously (1-3 e.g.). It is concerned both with the behavior and stability of thin liquid films upon simulated turbine blades under high velocity steam flow, and with their subsequent breakup into liquid droplets, which are then entrained into the wake giving rise to an erosion problem in the next downstream rotating row. The problem of thin liquid film behavior in the non-adiabatic case has application also to problems of "dry-out" in high void fraction boiling, particularly with regard to emergency core cooling of liquid-cooled nuclear reactors.

For this research program we have designed and constructed a low-pressure wet steam tunnel producing an approximately sonic velocity ($\sim$450 m/s) in a rectangular test section (8 cm x 8 cm) at a pressure of $\sim$3 psia. Simulated turbine blades, i.e., essentially thin flat plates, are inserted parallel to the flow direction along the axis of the test section (Fig. 1). In the case of this particular profile, with which the tests herein discussed were performed, 4 electrical conductivity liquid film gages were installed along the axis, evenly spaced. A liquid film is injected 3/4" upstream from the first gage. The behavior of this film, under adiabatic and diabatic conditions, is the primary subject of this report. The development and calibration of the gages was described previously (2,3); now their first use in actual high-velocity steam flow is reported.

II. EXPERIMENTAL FACILITY AND APPARATUS

A. Steam Tunnel Proper

The tunnel itself has been described previously (1-3, eg.) and some information is given above. Hence, only some additional especially pertinent features will be mentioned here.

1. Flow Instrumentation - Steam flow is measured both by pitot tube in the test section, and by an upstream orifice. The pitot tube is so positioned that it measures approximately the maximum steam velocity directly. The values so achieved should be quite reliable, since the test section pressure and temperature (steam is saturated) are essentially those of the condenser, and are held almost constant in our present mode of operation. On the other hand, the pressure and temperature at the orifice (intermediate between supply and test section conditions) vary considerably, depending upon the steam flow rate. However, due to the uncertain interpretation of a pitot tube data from high-velocity wet steam, the standard orifice data has been used in these tests. Steam flow rates calculated from the pitot tube are slightly greater than that from the orifice, because it measures approximately maximum velocity rather than average, as does the orifice.

2. Test Section Steam Conditions - Steam conditions in the test section are near saturation (never superheated), showing varying degrees of moisture depending primarily upon test section velocity (Table 1). Of course, wetness increases with velocity head for fixed supply conditions. It is assumed for the present purpose that supply conditions are constant, though this is of course not precisely true. No actual measurements of steam quality in the test section have been made (only conventional thermodynamic calculation), but precise knowledge of this parameter is not of great importance for the present purpose.

B. Blading Profiles

As reported previously (4,5 eg.), two symmetrical blading profiles of the same external geometry (Fig. 1) have been fabricated and used. A third profile (Fig. 2), also of approximately the same external geometry, has been fabricated, but not yet used in the tunnel. Hence it will not be discussed in detail here. The two blades, which have been used, differ only in that for #1, internal water cooling is used to induce condensation; and in #2 (Fig. 1), a water film is injected through a small slit normal to the tunnel axis.

The first two blades were tested previously (4,5) before the availability to us of the film thickness gages. Good still photographs of both of the condensed and injected liquid films were made, showing various surface wave formations and the shed droplet distribution in the wake. Since that time electrical conductivity film thickness gages have been installed in both blades #2 and #3, and calibrated under static conditions external to the tunnel (2,3,6). Blade #3, which provides for retrapping of the liquid film near the trailing edge to allow better study of liquid-vapor mass transfer, has not yet been tested in the tunnel. The primary subject of the present report is the test results upon blade #2, after the installation and calibration of the film thickness gages.

C. Electrical-Conductivity Thickness Gages

Details of the electrical conductivity film gages and their calibration are reported elsewhere (2,3). Only a few significant details will be given here. Essentially the electrical resistance* of a thin liquid film connecting the central pole of the gages with an external annulus (separated by an electrical insulator), all installed flush with the blade surface (Fig. 1-3),

*An aqueous solution with 0.5% NaCl (by mass) is used.

is measured by an a.c. circuit including a Wheatstone bridge. Output is to a dual-beam oscilloscope, so that the simultaneous output of two gages can be compared. The response time of the system is very fast so that the frequency and magnitude of local film surface waves can be measured. An a.c. circuit is used to avoid problems of electrostatic charge. While results depend somewhat on circuit frequency, it has been found that the response is flat with frequency in the range of 1 kHz, which is thus utilized. Two different gage models have been utilized and calibrated (Fig. 3). The difference is only in economy of fabrication cost. In both cases it is found that the output (in terms of circuit conductivity) is approximately linear for small film thicknesses, and that they essentially saturate at higher thicknesses (Fig. 4). Thus the useful operating range of the gages is limited, but sufficient to provide considerable useful data, as here reported.

III. EXPERIMENTS PERFORMED

A. Adiabatic vs. Diabatic Experiments

As a first approximation it is assumed that if the injected water film temperature is equal to that of the steam ($\sim$135°F, the experiment is adiabatic. This has been the case for most of the tests, but in some cases cold water has been used ($\sim$65°F). Steam temperature is always T_{sat}, which is approximately the same for all runs due to maintenance of constant condenser conditions. For cold water injection it is assumed that significant steam condensation will occur, and hence the liquid film thickness increase. This expectation has been generally fulfilled as discussed later.

B. Range of Steam Velocity and Film Injection Rate

1. Steam Velocity

As mentioned in various previous reports the maximum steam velocity is about sonic ($\sim$450 m/s or $\sim$1400 f/s). This is necessarily the case,

since to the present no good diffusing section has been attached after the constant area rectangular test section. Total available pressure ratio between supply line and condenser is ~6, but of course much of this is used in the system ahead of the test section. Nevertheless, the pressure available for the converging nozzle immediately upstream of the test section is adequate to provide approximately Mach 1 at this point. Higher Mach numbers may be investigated at a later date with the installation of a properly designed diffusing section after the test section.

There is no limiting minimum velocity which can be precised other than by ability to measure it with adequate precision. The minimum velocity so far used has been ~100 f/s. Very low velocities are desirable for the investigation of liquid film stability as will be discussed later.

2. Film Injection Rate

As previously mentioned the liquid film is injected through a narrow slot across the blade (Fig. 1), near its leading edge. Minimum film injection rate depends upon the presently available measuring and throttling capability, and is ~5 cc/m. Maximum meaningful injection is set by the spraying and jetting of the film which occurs at high injection rates. A present meaningful maximum rate is ~60 cc/m. The pressure differential for film injection is primarily due to the "vacuum" in the test section (~3 psia exists there) plus a few feet of elevation head due to the location of the film-liquid bottle, which is open to atmosphere. Hence larger injection rates could easily be achieved if desired.

C. Visual Appearance of Film and Shed Droplet Spectrum

Visually (by strobe light or photographically), and from the output of the thickness gages (discussed later), the film thickness is in general not uniform in time or space, and in fact often includes an apparently complex wave pattern. Also at some times "dry spots" and/or an axial filament flow pattern have been observed. Miscellaneous photographs (~1 μs exposure) which we have previously reported (3,4, eg), taken from earlier tests (before installation of thickness gages) on blades #1 and #2 (Fig. 1) are typical for the appearance of the film (both injected and condensed upon cooled blade) and for the downstream droplets (Fig. 5 and 6). Figure 6-b in particular shows apparent film breakdown into dry spots and filaments, occurring just before the downstream tapered section of the blade for a condensed (non-injected) film, at approximately maximum steam velocity. Unfortunately, film thicknesses are not available for these photos, since the gages were not available at that point. In these cases, the film breakdown appears to be provoked by small screw heads in the blade surface which may not have been entirely flush with the blade surface.

Later tests upon blade #2 have also showed such breakdown into filaments, at minimum steam velocity and injected film flow rate, near the injection slit. Unfortunately, no photographs are yet available from these tests.

Figures 5 and 6 also show typical entrained droplet spectra in the blade wake. The larger drops were ~0.055 - 0.11 mm diameter, and no doubt originate from the liquid film upon the blade, since droplets formed within the steam should theoretically be no larger than ~1 μm (7, eg.). No downstream droplet photos from the more recent tests are yet available.

Figure 5-a,b shows apparent back-flow on the trailing tapered portion of the blade, perhaps induced by the slight adverse pressure gradient in this region due to the increased flow area (due to taper). This type of flow phenomenon may contribute to increased film thickness noted by the downstream gages, discussed later.

D. Film Thickeness Measurements

The film thickness gages (Fig. 1 and 3) produce instantaneous film thickness measurements at four evenly spaced locations along the axis of the upper blade surface. Hence time average as well as time dependent thicknesses are provided. The existence of 4 gages spaced axially allows also a measurement of film thickness variation along the blade.

The time average values can of course be directly related to the axial shear between steam and liquid, assuming the liquid film flow to be laminar, thus producing a classical uniform shear Couette flow, where film velocity varies linearly with distance from blade surface. Since maximum computed film velocity is only $\sim$ 0.1 f/s and thickness only a few mils (Re $\tilde{=}$ 40) the assumption of laminar flow in the film is well justified. The steam flow is of course generally well within the turbulent range, so that shear from the viewpoint of the steam side must be estimated from conventional friction factor data (steam axial pressure drop is essentially only that of friction, and too small for accuraate measurement). As discussed later, measured film thicknesses and those computed from considerations of film shear agree well in terms of trends, but a presently unexplained absolute discrepancy exists.

Instantaneous film thickness measurements can shed some light on the surface wave formations in the liquid film. Proportionate thickness variation is discussed and presented later. Also, wave frequency can be

deduced from the oscilloscope photos obtained (discussed later). Wave velocity can only be found when actual photos of the wave surface under conditions wherein the wave frequency has been measured. From such photos, wave-lengths can be estimated, and then wave velocity computed from the relation: $C_w = f \lambda$ ..... (1)
Unfortunately these photos have not as yet been obtained, but hopefully will be available in the fairly near future.

IV. RESULTS - EXPERIMENTAL AND THEORETICAL

A. Steady-State (Time Average) Results

1. Theoretical Treatment

As briefly explained previously, the total flow regime including both high velocity steam and liquid film can be analyzed on the assumption that equality of axial shear exists between steam and liquid at the interface. Since steam pressure is approximately uniform through the test section (no acceleration pressure drop), the steam friction drop can be directly related to the interface shear. Since this pressure differential is too small for meaningful measurement, it can only be estimated through conventional fluid friction pressure drop calculations using the concepts of hydraulic diameter and friction factor, where f = f(Re). Unfortunately, experimental data is limited to flow with solid walls with known roughness, so that the effective friction factor between liquid and gas is not well known. This fact may be primarily responsible for the mismatch of film thickness data between calculation and gage measurements, discussed later. The full details of our data reduction procedures in this and other matters are presented in a separate report (8).

Interface shear can be related to the thin liquid film flow regime assuming it to be a constant shear Couette flow with linear velocity profile

$$V_{liq_{max}} = \tau (h/\mu_{liq}) \quad \ldots\ldots\ldots\ldots\ldots\ldots\ldots \quad (2)$$

The continuity equation can also be applied for the liquid flow to give a relation between the injected flow rate, $\dot{m}$, the film thickness, h, and the maximum liquid axial velocity (at the steam-liquid interface), assuming adiabatic flow with no evaporation or condensation, i.e.,

$$\dot{m}_{liq} = \rho \bar{V}_{liq} A_{liq} = \rho (V_{liq_{max}}/2) bh \quad \ldots\ldots\ldots \quad (3)$$

where b is blade width.

Combining Eqs. (2) and (3), interface shear, τ, can be related to h for curves of constant $\dot{m}$. τ can also be computed for fixed test section steam conditions as a function of steam velocity, V_{steam}. It is then obviously possible to relate film thickness, h to test-section steam velocity, V_{steam} with $\dot{m}$ as curve parameter, thus obtaining a theoretical prediction for film thickness for fixed flow test parameters. These can then be checked against measured film thicknesses (Fig. 7-13). The full details of the data reduction for both predicted and measured film thickness is given elsewhere (8).

2. Experimental vs. Theoretical Film Thickness-General

Figure 7 summarizes the theoretical expectations concerning film thickness as a function of steam velocity for different injected liquid film flow rates. Two major trends are shown, i.e, film thickness, h decreases for increasing steam velocity (more strongly at small steam velocity), and it increases for increasing injected film flow rate. The anticipated effect with increasing film injection rate is intuitively obvious, and that with steam velocity can be explained on the basis that increasing V_{steam} means increased interface shear, which means increased $\partial V/\partial y$ for the liquid; hence increased liquid velocity, and reduced film thickness. These curves (Fig. 7) are drawn on the assumption of temperature equality between steam

and water at T_{sat} for the condenser conditions. Actual temperature and pressure measurements approximately confirm this assumption. Thus the curves reflect adiabatic flow conditions, since in addition no mass transfer between steam and liquid was assumed.

Figure 7 also includes a curve for $h_{crit.}$, the critical film thickness, where according to the most recent analysis (based on the conservation of kinetic and surface energy) it could desintegrate into individual axial liquid filaments (9). This question will be discussed in detail later.

Figures 8-13 compare measured film thicknesses with those theoretically predicted (as explained above) for different film injection rates. No differenti tion between points for different axial positions is made here. In all these cases there is approximate temperature equality between steam and liquid, so that the process is essentially "adiabatic". In general the experimental data confirms the two major trends predicted theoretically, i.e., increasing film thickness for increasing film injection rate and decreasing steam velocity. While there is much experimental scatter and also constant high frequency oscillation of the thickness gage output (discussed later), the "best curves" for the experimental data show film thicknesses about 2 x those expected theoretically. Considering that it is a question of an "error" in film thickness measurement of only a few mils, and that there are many possibly considerable sources of error in the reduction of both theoretical and experimental data, the degree of agreement achieved, rather than the discrepancy, may be the more remarkable. However, at this point we have no specific explanation for the systematic discrepancy found. Of course, it could be interpreted as the result of a mis-estimation of the friction factor, f. To explain the present results in this fashion, f would need to be reduced by $\sim$ 2 x. This seems unlikely to be the actual case, since "hydraulically smooth" walls were already assumed. However, published f-values are based

upon flow through pipes with solid walls, and to our knowledge, no actual friction measurements for interfacial fluid friction pertinent to the present case exist. Of course, the apparent surface waves should increase the friction, making unlikely the existence of very small friction factors in the present case.

3. Effect of Axial Position

Figures 14-19 show the variation with axial position along the blade of film thickness for the different steam velocities used at the different film injection rates. Again much data scatter is noted, but the trend generally persists that the 3rd gage position (somewhat downstream of axial midpoint of blade) shows a maximum thickness, and the 2nd gage position (somewhat upstream of axial midpoint) a minimum film thickness. This may indicate the existence of relatively stationary standing surface waves in the film, but no definite statements in this regard can be made until good film photos are obtained. An attempt to investigate the possibility of measuring wave speed by instantaneous oscilloscope photos (using a dual-beam scope) of the output of different gages was inconclusive. However, this technique may be attempted again in the future.

The existence of an increased film depth for the downstream portion of the blade might be due to "piling up" and back-flow of the film in this portion, due to the adverse steam pressure gradient in this region, which in turn is due to the trailing edge blade taper. Earlier film photos (Fig. 6) tended to indicate this possibility, as previously mentioned.

The theoretical treatment (already explained) which is based upon steady-state behavior and considers no surface wave formation, provides no explanation for the observed differences in film thickness with axial position (Fig. 14-19). "Entry effects" for the film flow would not be expected to have an observable influence, since the effective L/D for the film is very large, since h is

only a few mils, so that it must be assumed that the film is "fully developed" at all gage stations. Of course some "entry effects" for the steam flow may exist, and its boundary layer thickness may increase considerably axially along the blade, since the effective L/D for the steam flow is ~ 2. Whether or not this would influence the liquid film thickness appreciably is a matter for further analysis. However, the influence appears to be in the right direction, since increased shear would exist for the upstream portion, there thinning the film, as observed.

4. Adiabatic vs. Diabatic Conditions

For the data so far discussed, the tests have been essentially "adiabatic" in that the injected film temperature and that of the steam in the test section have been maintained equal as closely as possible. However, a series of cold ($\sim 65°F$) water film injection tests has also been performed. These tests are "diabatic", and provoke heat and mass transfer from the steam to the film. For purposes of reduction of film thickness gage output, it is assumed that the film temperature remains as injected (8). A more detailed theoretical study of the total flow steam-water regime with heat and mass transfer to verify or disprove the validity of this assumption has not yet been made.

Figures 20-21 are similar to Figs. 7-13, except that they are for the diabatic cold water tests. The dependence of the theoretical film thicknesses on steam velocity and injected film flow rate is approximately as before (8); however, the measured film thickness dependence upon steam velocity appears much greater even though data so far gathered is relatively fragmentary. In fact, for maximum steam velocity the thickness is often below the useful range of the gages (apparently only small fraction of a mil), and for low steam velocity the thickness may be too great for accurate measurement with these gages,

as their output "saturates" at somewhat lower thickness. It is thus only in the intermediate steam velocity range that good agreement can be obtained. However, in general the film thickness is essentially asymptotic to zero at high steam velocity and becomes very large (perhaps $>$ 10 mils) at low velocity (Fig. 21).

Measured large film thickness at low steam velocity (as compared to adiabatic tests) is to be expected due to the increased condensation from the steam. This effect can be expected to be less at higher steam velocities. This would provide greater heat transfer at higher steam velocity (increased heat transfer coefficient) so that the thin liquid film would approach steam temperature. From this viewpoint the tests should become identical with the adiabatic tests under maximum steam velocity. In most cases the measured film thickness is $<$ 1 mil at maximum steam velocity. However, it often approaches $\sim$ 0.1 mil for the cold water tests. Of course it may be foolish to place any credence in indicated thickness differences of such small absolute magnitude. However, no theoretical justification for this difference between the tests at the high velocity extreme is apparent. After more detailed flow analyses have been completed some explanation may be afforded, and this will hopefully be covered in a later report. Of course the thickness measurements roughly agree in the intermediate steam velocity range, since the discrepancies are in different directions at the extremes.

5. Critical Film Thickness for Breakdown into Axial Filament Flow

a. General Background

Numerous observations of the flow of thin liquid films driven either by gravity or by shear with a high-velocity gas stream (as in the present case) have shown breakdown of the simple laminar Couette flow in various ways, including surface waves and breakdown into axial liquid filaments or other "dry spots". These phenomena are of course of much importance in many technological applications. Numerous theoretical predictions of film breakdown have accompanied these observations (10-22). The earlier analyses (11-17 e.g.) were based on small perturbation techniques, and hence can perhaps not be expected to give accurate results for the very large perturbations corresponding to film breakdown. Later analyses (18-22, eg) are based upon different more comprehensive physical models, the details of which are beyond the scope of the present report. One of the latest approaches, that by Mikielewicz and Moszynski (9,10) has been here used for comparison with our observations. This model, based on the conservation and minimization of kinetic and interfacial tension energies, appears to give results closest to the present observations (23 and is hence used for comparison with our experimental data.

b. Present Results

As previously mentioned, critical film thickness lines from this analysis (9) have been plotted on the curves showing experimental and theoretical film thicknesses (Fig. 7-13). These critical thickness lines were computed for a wetting angle of 70°, since preliminary experiments using photographs of droplets upon our blading surface (Fig. 22) show this value to be appropriate. The critical film thickness depends upon wetting angle to some extent (Fig. 23-24 but not enormously within the plausible range of wetting angles.

Figures 7-13 indicate that by and large the critical film thicknesses lie well above the observed data points which do not themselves include film-filament transition. According to the analysis, however, film-filament breakdown could occur energetically for the entire regime of film thickness vs. steam velocity below the h_{crit} curve. The analysis does not of course indicate that it will occur unless the flow is sufficiently perturbed. The photographs of Fig. 6 indicate that such a transition can occur in the wake of a small surface perturbation (screw-head in this case). Hence tests to observe the effect of small obstructions, and the behavior of the film downstream of these, would be most instructive, and are planned for the near future.

For most of the operating range investigated some degree of breakdown of the simple Couette flow has been observed as indicated by oscilloscope pictures of gage output (Figure 25), to be discussed later. However, actual film-filament transition has been observed only downstream of an obstruction (Fig. 6, maximum steam velocity, film thickness unknown), and also for very low steam velocity ($\sim$ 100 f/s), minimum film injection rate, film thickness unknown. This latter case was only a random observation, which has not yet been further investigated or photographed. Hence it appears at this point that the film thickness, steam velocity regime for film-filament transition is very much lower, in terms of film thickness, than that predicted by the present theory (9) perhaps by $\sim$ 5-10 x.

B. Time Dependent Results

The previous discussions have all considered only time average gage outputs. However, since the gages provide a very high response rate, much meaningful information can be gleaned from their time-dependent output, as will be discussed below.

Figure 25 shows oscilloscope photos of thickness gage output. The distance across the photos is proportional to the gage circuit resistance, and from this the instantaneous and average film thicknesses can be obtained (8).

The photo-band envelope height at a given instant is the value sought, not the individual "carrier wave" peaks, which derive from the imposed 1 kHz circuit frequency. Overall envelope waves are then the waves of interest. Both their magnitude and frequency can be found from examination of the scope photos, as discussed below.

1. Film Thickness Variation with Time

Figure 25 shows typical scope pictures of gage output, from which magnitude of thickness variation from the mean, h, and average film thickness, $\bar{h}$ can be obtained. The quotient of these represents the mean-to-peak wave height divided by average depth, i.e., the relative wave height. Present data is very scant but a typical value for $h/\bar{h}$ is 0.75.

2. Surface Wave Frequency

Surface wave frequencies have been estimated from the scope pictures of thickness gage output and plotted against V_{steam} in Figure 26. Typical frequency of the surface oscillation is $\sim$10 Hz. These waves will be the subject of more detailed future study than has so far been possible in that the study of their actual nature should enhance the ability to predict film breakdown into "dry spots", filaments, or whatever transition may actually occur.

Surface wave propagation velocity cannot be inferred from the present data, since no measurements of wave length have been made. This parameter can only be obtained from actual photos of the film surface itself under condition where wave frequency and the other pertinent parameters were measured. Because the wave frequency measurement requires the thickness gage output, the earlier film photos (Fig. 5 and 6) cannot be used in this respect. Once wave length has been estimated, wave propagation velocity can be computed from eq. (1)

V. CONCLUSIONS

Some principal conclusions can be drawn from this preliminary experimental and theoretical study of liquid film thickness along a flat blade immersed parallel to a high-velocity, low-pressure, wet-steam flow. Since the present report emphasizes particularly the documenting of observations and data obtained to date, it is likely that more careful analyses both of measurements and theory will provide additional important conclusions from these same tests. These will be covered in future reports.

1. Measured (average) liquid film thicknesses agree qualitatively very well with thicknesses computed from considerations of interfacial shear between high-velocity steam and low-velocity liquid based on test section estimated friction factors, assuming liquid film to be laminar, uniform and steady-state, and assuming the tests to be adiabatic, since injected film and steam temperatures are equal. The laminar assumption appears to be well justified, but the thickness gage output indicates that the film is not uniform or steady-state, rather exhibiting numerous relatively high-frequency ($\sim$ 10 Hz) surface waves. No steam axial pressure drop data was used, since it is too small for accurate measure.

   Qualitative agreement between measured and calculated film thickness has been obtained in that the proportionate film thickness decreases with steam velocity and reduced injected film flow rate roughly in the proportions as predicted. Quantitative agreement is relatively poor in that the predicted thicknesses are $\sim$ 1/2 those actually measured. No explanation, other than the obvious uncertainty of friction factor between wet steam and liquid surface, exists. However, friction factors $\sim$ 1/2 those for hydraulically smooth pipe would be necessary to achieve agreement, and this does not seem a realistic possibility at this point.

2. Low temperature film injection tests (diabatic conditions) produced markedly thicker films at low steam velocity as would be expected due to the effect of steam condensation. The effect of cold water injection (compared to steam temperature water) at moderate steam velocity upon film thickness was nil, probably because the higher steam velocity, and hence greater heat transfer coefficient between steam and water, allowed the liquid film to increase to approximately that of the steam. At maximum steam velocity the measured film thicknesses for cold water injection were less than those for hot water, for reasons presently unexplained. A more detailed analysis of the overall flow regime, including heat and mass transfer effects, may be necessary to further explain these results.

3. Systematic variation of film thickness with axial position along the blade was observed, with film thickness peaking in the downstream portion of the blade. This apparent existence of standing surface waves along the blade must be further investigated using photographs of the actual film surface. More detailed analysis of the overall flow regime may also help in this regard.

4. Numerous theoretical predictions of film breakdown into axial filaments or other "dry spots" have been made in recent years. However, our present data shows such breakdown only for much lower film thicknesses and steam velocities than those predicted. The error in terms of film thickness is by a factor of $\sim$ 5-10. This situation must be the subject of continued experimental and theoretical investigations.

5. Complex surface wave patterns have been observed in the present and past tests in our tunnel. Wave frequency has been measured to be $\sim$10 Hz. Since no wave length measurements have yet been obtained, it is not yet possible to estimate wave velocity.

References

1. J. Krzyzanowski, "Wet-Steam Tunnel Facility - Design and Program of Investigations," ORA Report No. UMICH 03371-18-T, June 1972.

2. J. Mikielewicz, F.G. Hammitt, "Generalized Characteristics of Electrical Conductanc Film Thickness Gauges," ORA Report No. UMICH 012449-7-I, December 1974.

3. F.G. Hammitt, J. Mikielewicz, G. Ernst, D. Krause, L. Rockwell, "Steam Tunnel Program and Liquid Film Thickness Gauge Developments at University of Michigan," ORA Report No. UMICH 012449-6-T, January 1975.

4. F.G. Hammitt, A. Keller, G. Ernst, "Steam Tunnel Initial Operation and Results," ORA Report No. UMICH 012449-1-T, January 1974.

5. F.G. Hammitt, A. Keller, G. Ernst, "Low-Pressure, Wet, Steam Tunnel - Initial Results," ORA Report No. UMICH 012449-1-I, January 1974.

6. F.G. Hammitt, "Wet Steam Tunnel - Progress Report No. 1," ORA Report No. UMICH 012449-1-PR, March 1975.

7. R. Puzyrewski, T. Krol, "Numerical Analysis of Hertz-Knudsen Model of Condensation Upon Small Droplets in Water Vapor," Proc. Inst. Fluid Flow Machinery, Polish Academy of Science, Gdansk, Poland, 1970.

8. A. Mancuso, etal., "Data Reduction Procedures - Steam Tunnel Film Thickness Tests," ORA Report No. UMICH 012449-20-I, June 1975.

9. J. Mikielewicz, J.R. Moszynski, "Breakdown of a Shear Driven Liquid Film," to be published, Proc. Inst. of Fluid Flow Machinery, 1975.

10. J. Mikielewicz, J.R. Moszynski, "Minimum Thickness of a Liquid Film Flowing Down a Solid Surface," submitted to Int. J. Heat and Mass Transfer.

11. V.A. Hallett, "Surface Phenomena Causing Breakdown of Liquid Films During Heat Transfer," Int J. Heat and Mass Transfer, 9, 1966, p. 283.

12. J. Mikielewicz, "On Evaporation and Stability of Water Films on Heated Guide Blades of Steam Turbines," (in Polish), Trans. Inst. for Fluid Flow Machines, Polish Academy of Science, 1974, nr. 64, p. 79.

13. S.G. Bankoff, "Stability of Liquid Flow Down a Heated Inclined Plane," Int. J. Heat and Mass Transfer, 14, 1971, p. 377.

14. A.A. Zajcew, "On Waves on the Surface of a Viscous Film Driven by a Steady Shear Stress," (in Russian) Vestnik Moskowskogo Universyteta, 1960, 2.

15. W.B. Krantz, S.L. Goren, "Stability of Thin Liquid Films Flowing Down a Plane," Ind. Eng. Chem. Fundam., 10, 1971, 1, p. 91.

References (cont.)

16. B. Anshus, "On the Asympotic Solution to the Falling Film Stability Problem," Ind. Eng. Chem. Fundam., 11, 1972, 4, p. 502.

17. A.H. Nayfeh, W.S. Saric, "Stability of a Liquid Film," AIAA Journal, 9, 1971,

18. D.E. Hartley, W. Murgatroyd, "Criteria for the Breakup of Thin Liquid Layers Flowing Isothermally Over a Solid Surface," Int. J. Heat and Mass Transfer, 7 1964, p. 1003.

19. G.F. Hewitt, P.M.C. Lacey, "The Breakdown of the Liquid Film in Annular Tv Phase Flow," Int. J. Heat and Mass Transfer, 8, 1965, p. 781.

20. W. Murgatroyd, "The Role of Shear and Form Forces in the Stability of a Dry I in Two-Phase Film Flow," Int. J. Heat and Mass Transfer, 8, 1965, p. 297.

21. A. Orell, S.G. Bankoff, "Formation of a Dry Spot in a Horizontal Liquid Film I from Below," Int. J. Heat and Mass Transfer, 14, 1971, p. 1835.

22. N. Zuber, E.W. Staub, "Stability of Dry Patches Forming in Liquid Films Flov Over Heated Surfaces," Int. J. Heat and Mass Transfer, 9, 1966, p. 897.

23. G. Moszynski, personal communication to F.G. Hammitt, May 1975.

TABLE 1

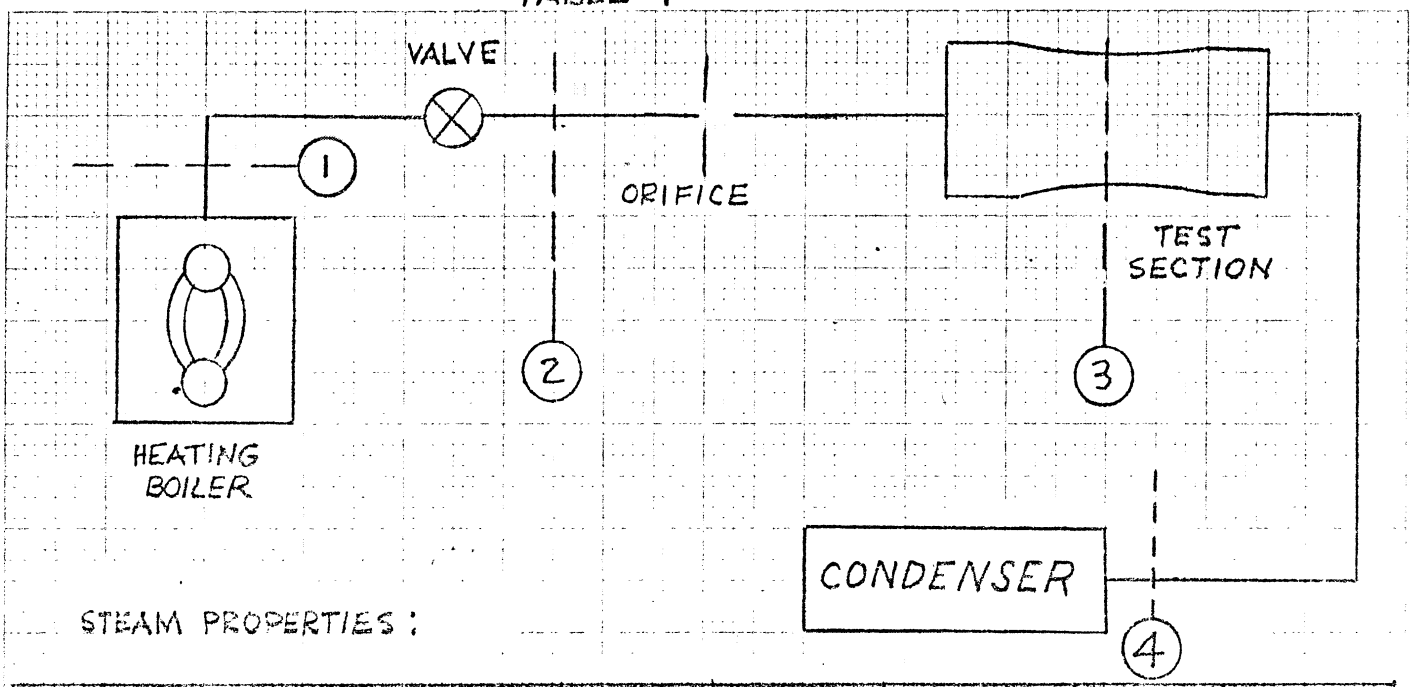

STEAM PROPERTIES:

V_{STEAM} (FT/SEC)	T_3 (°F)	P_3 (lb/in²)	h_3 (BTU/lbm)	S_3 (BTU/lbm)	X_3	T_1 (°F)	P_1 (lb/in²)	X_1	h_1 (BTU/lbm)	S_1 (BTU/lbm)
200	130	2.225	1107.456	1.894	.99	227.96	20	.95	1108.255	1.662
600	↓	↓	1101.065	1.877	.98	↓	↓	↓	↓	↓
1500	↓	↓	1063.316	1.825	.95	↓	↓	↓	↓	↓

NOTE: Conditions at "3" and "4" approx. same.

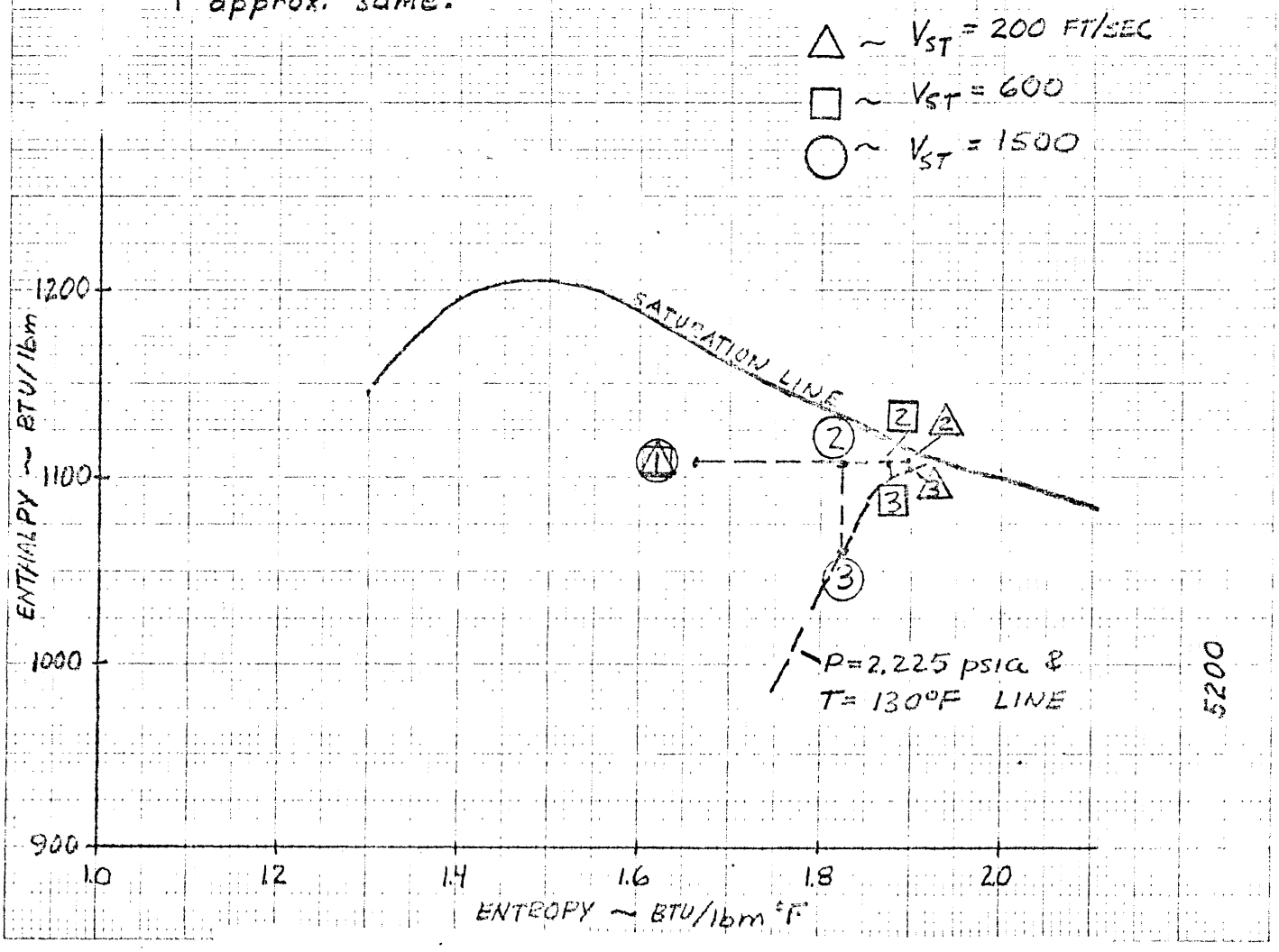

1. Thermodynamic Operating Conditions of Steam Tunnel

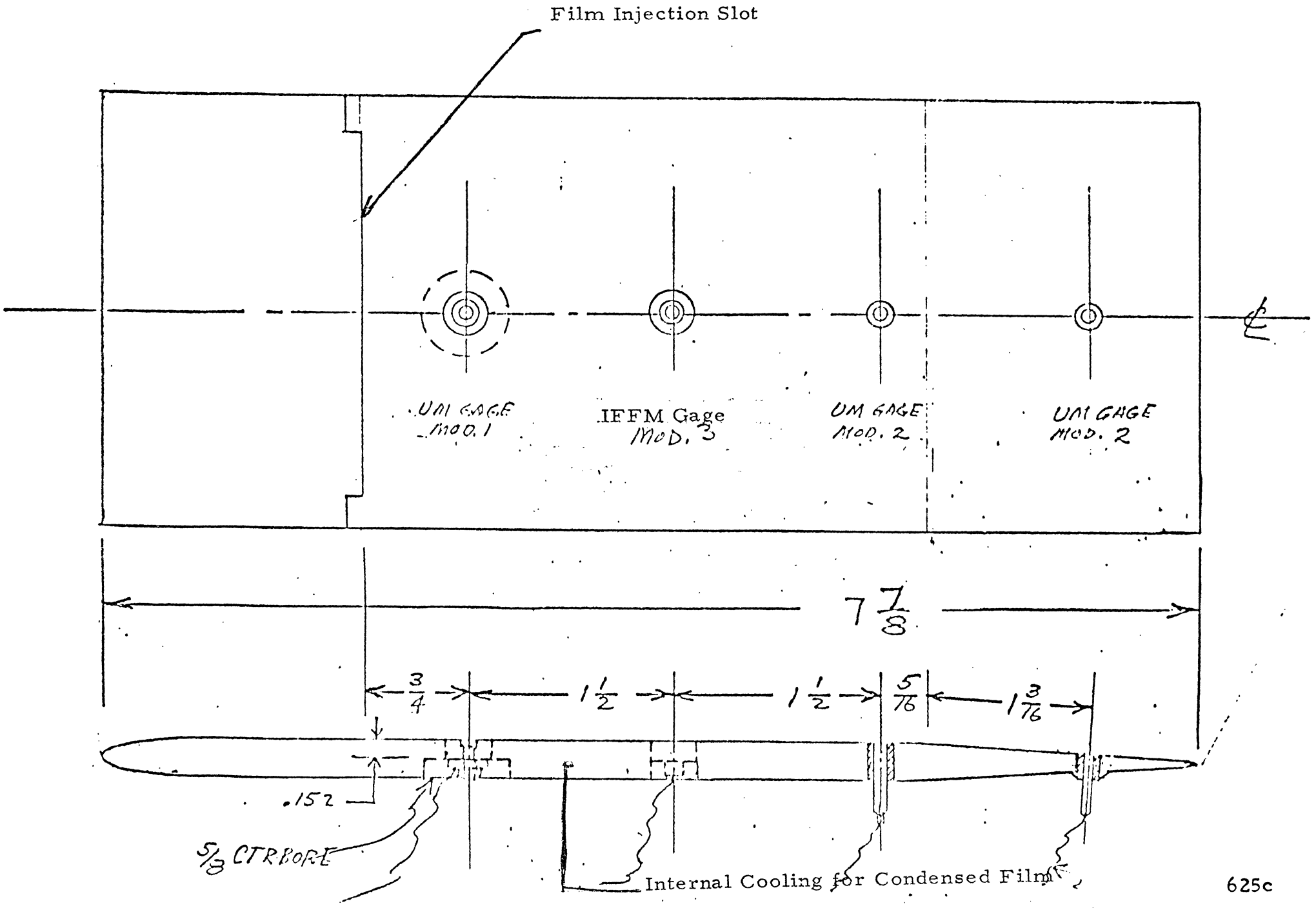
Film Injection Slot
UM GAGE MOD. 1
IFFM Gage MOD. 3
UM GAGE MOD. 2
UM GAGE MOD. 2
7 7/8
3/4
1 1/2
1 1/2
5/16
1 3/16
.152
5/8 CTRBORE
Internal Cooling for Condensed Film

625c

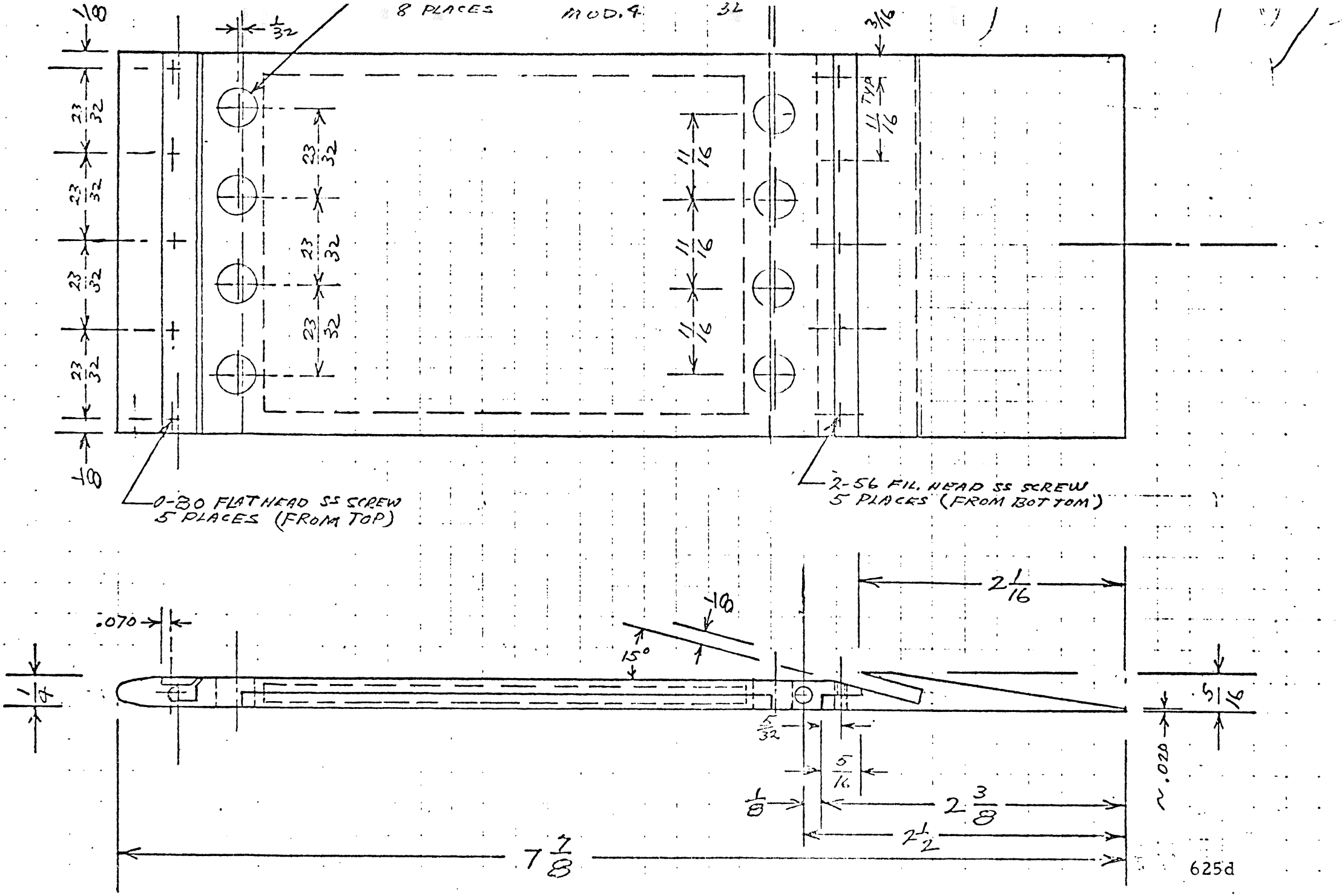

2. Blade Profile No. 3 (Film Recovery Blade)

3. Electrical Conductivity Gages

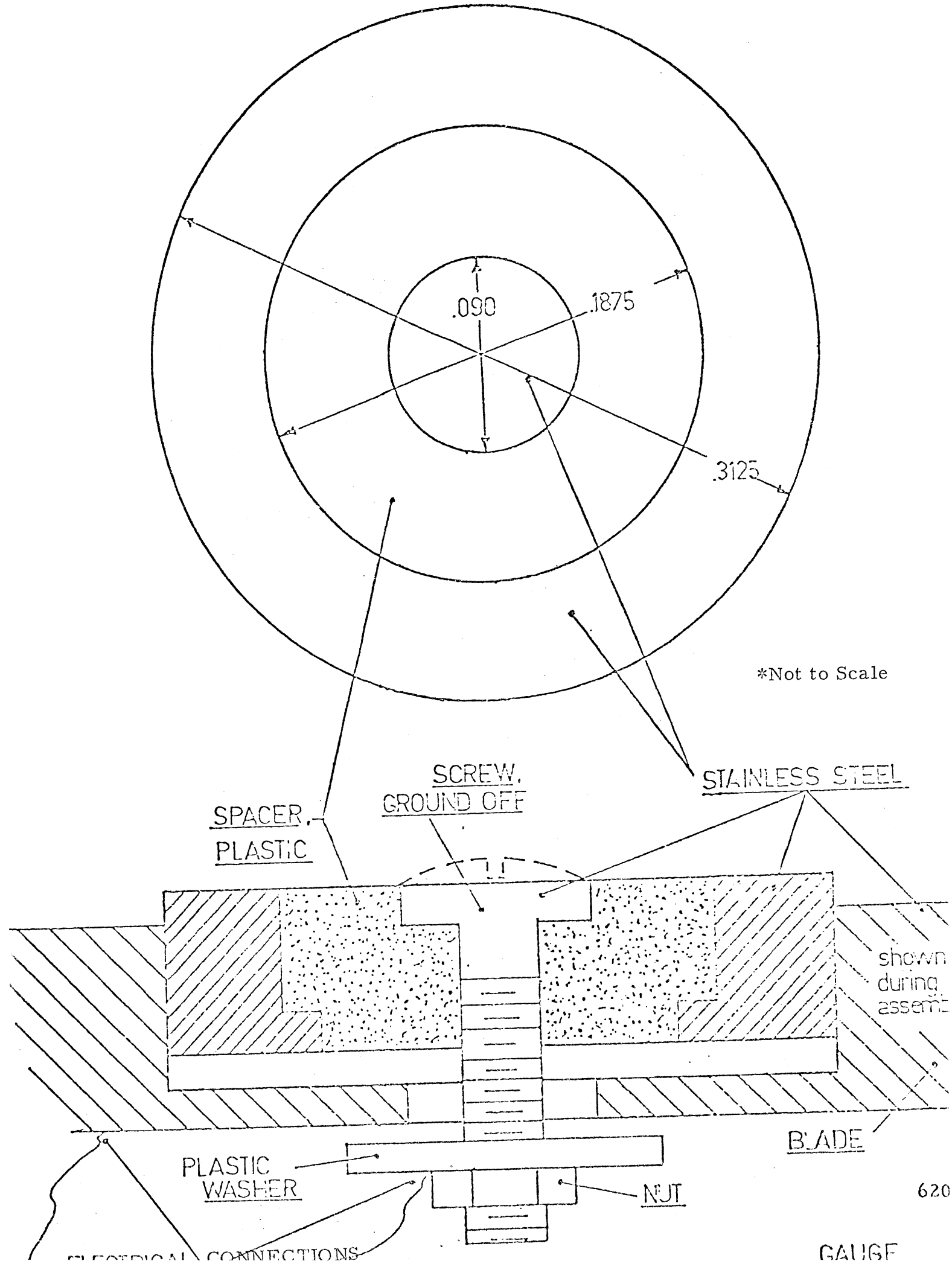

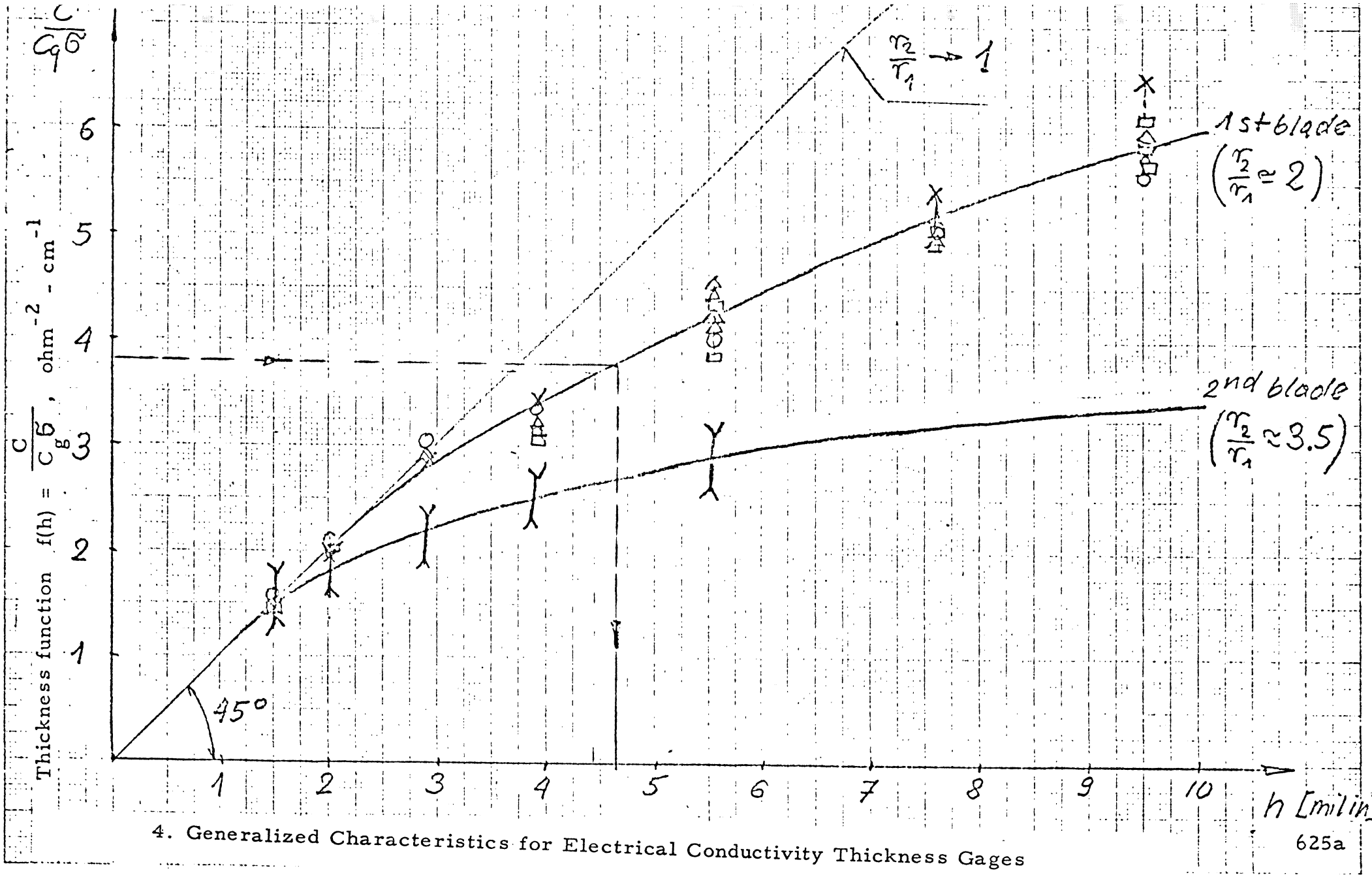

4. Generalized Characteristics for Electrical Conductivity Thickness Gages

625a

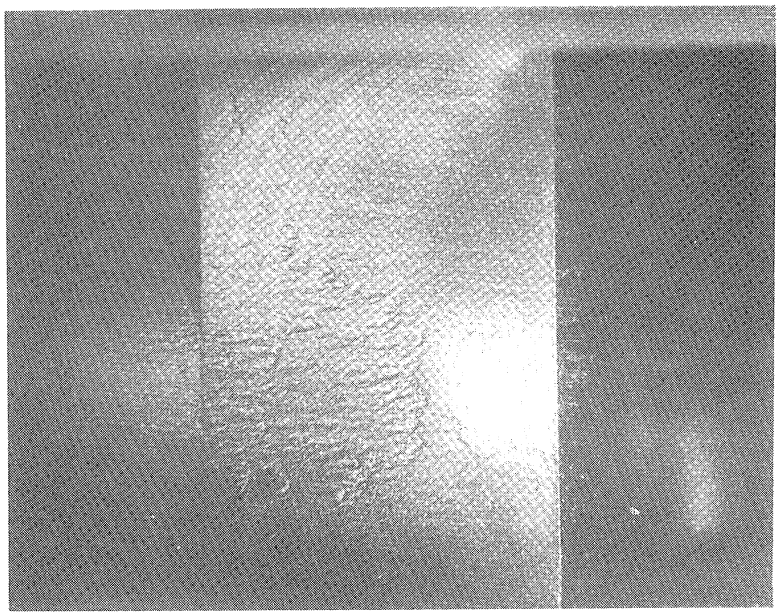

a. 20 cc/min.

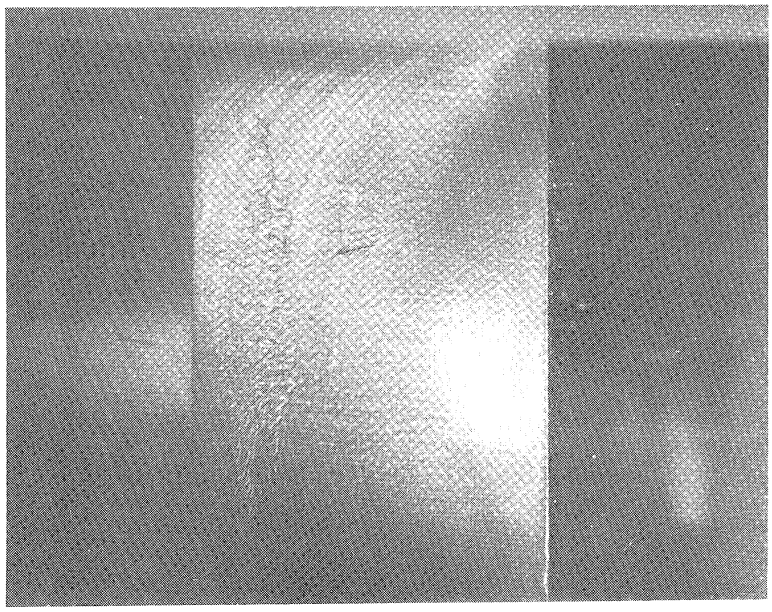

b. 10 cc/min.

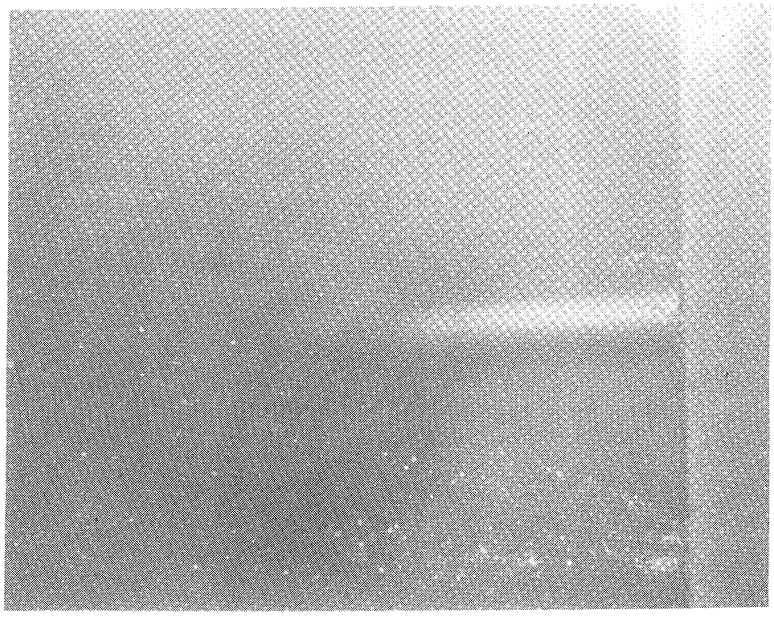

c. 30 cc/min.

5. Film and Droplet Photos - Injected Water Film (Blade Profile No. 2)

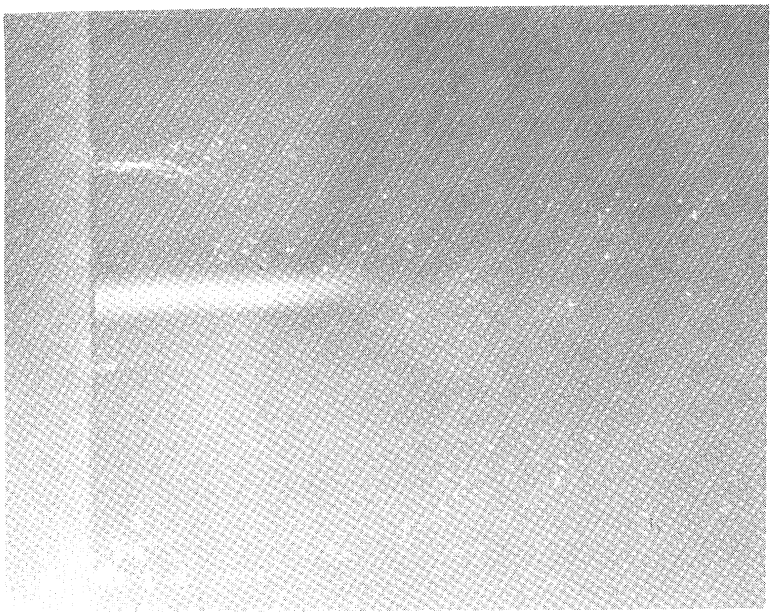

a. Injected Water Film,
Steam Velocity = 229 m/s,
Film Flow Rate = 21 cc/min.

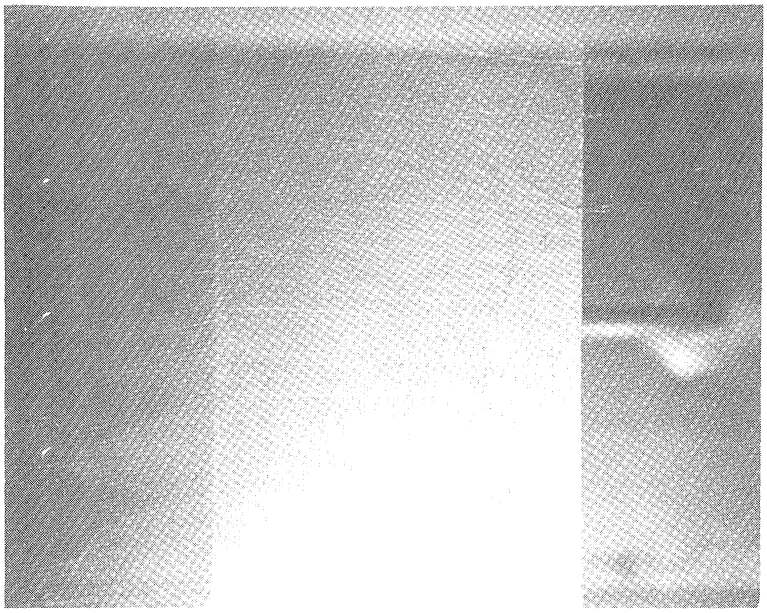

b. Cooled Blade, Condensed Water
Film. Steam Velocity = 415 m/s,

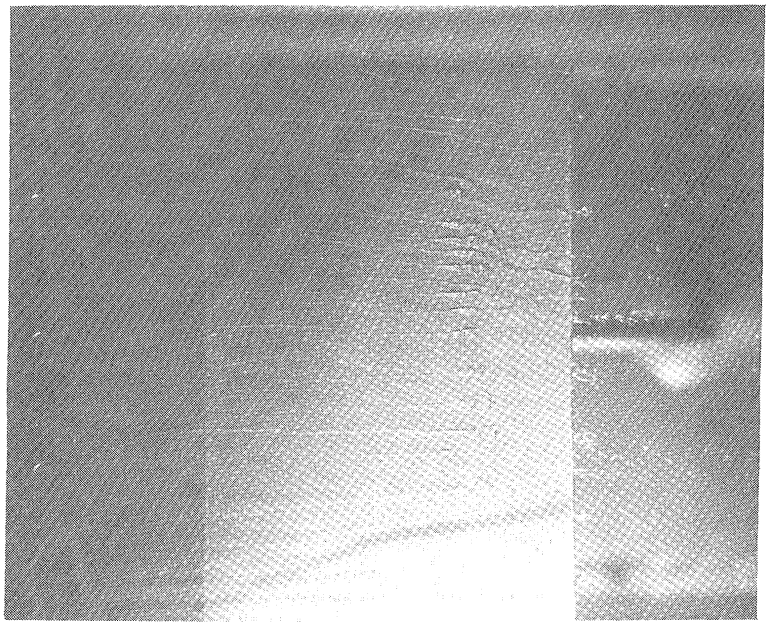

c. Cooled Blade, Condensed Water
Film, Steam Velocity = 415 m/s,

6. Film and Droplet Photos - Injected and Condensed Films (Blade Profiles No. 1 and 2

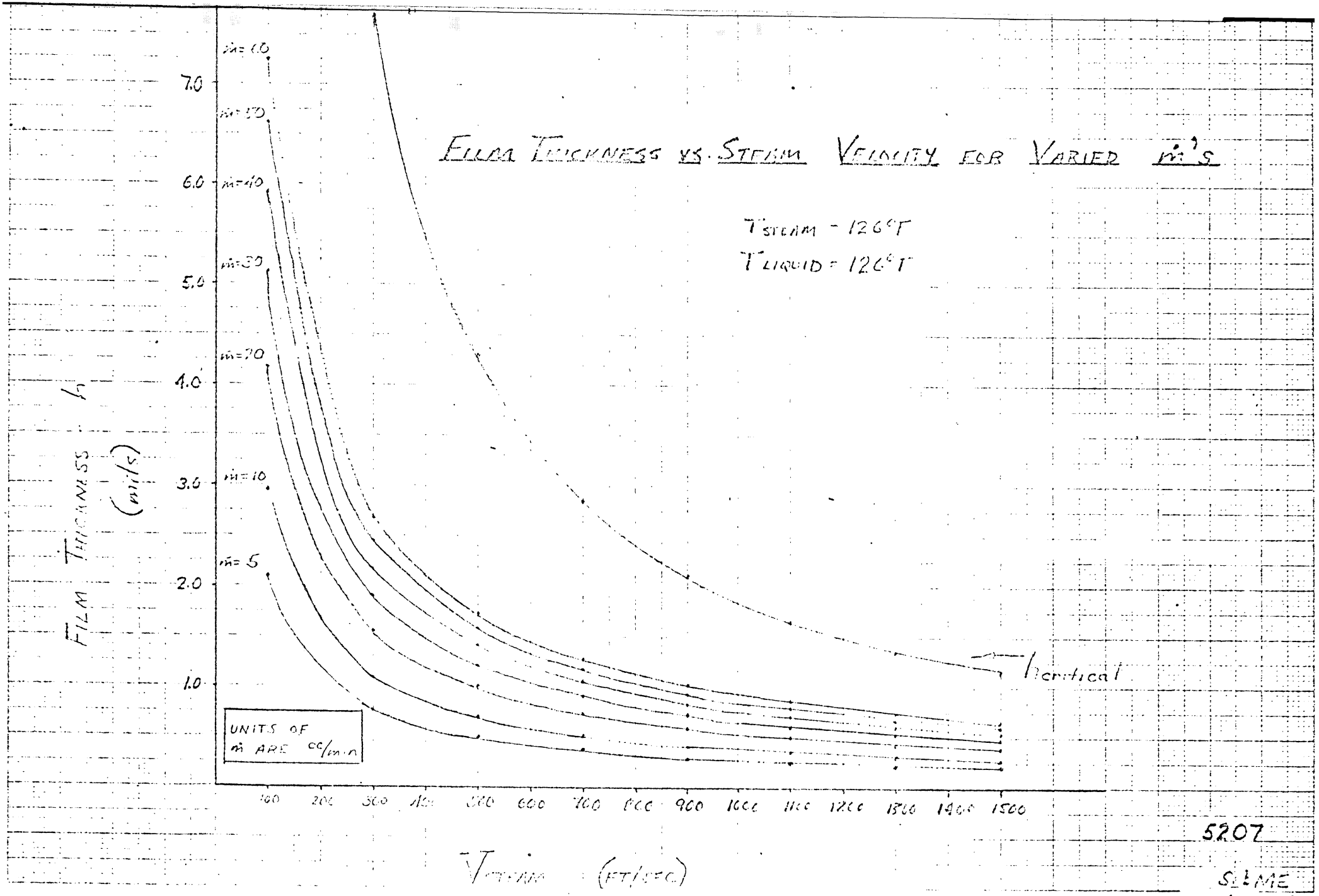

7. Predicted Adiabatic Film Thickness vs Steam Velocity; Various Liquid Film Flow-Rate

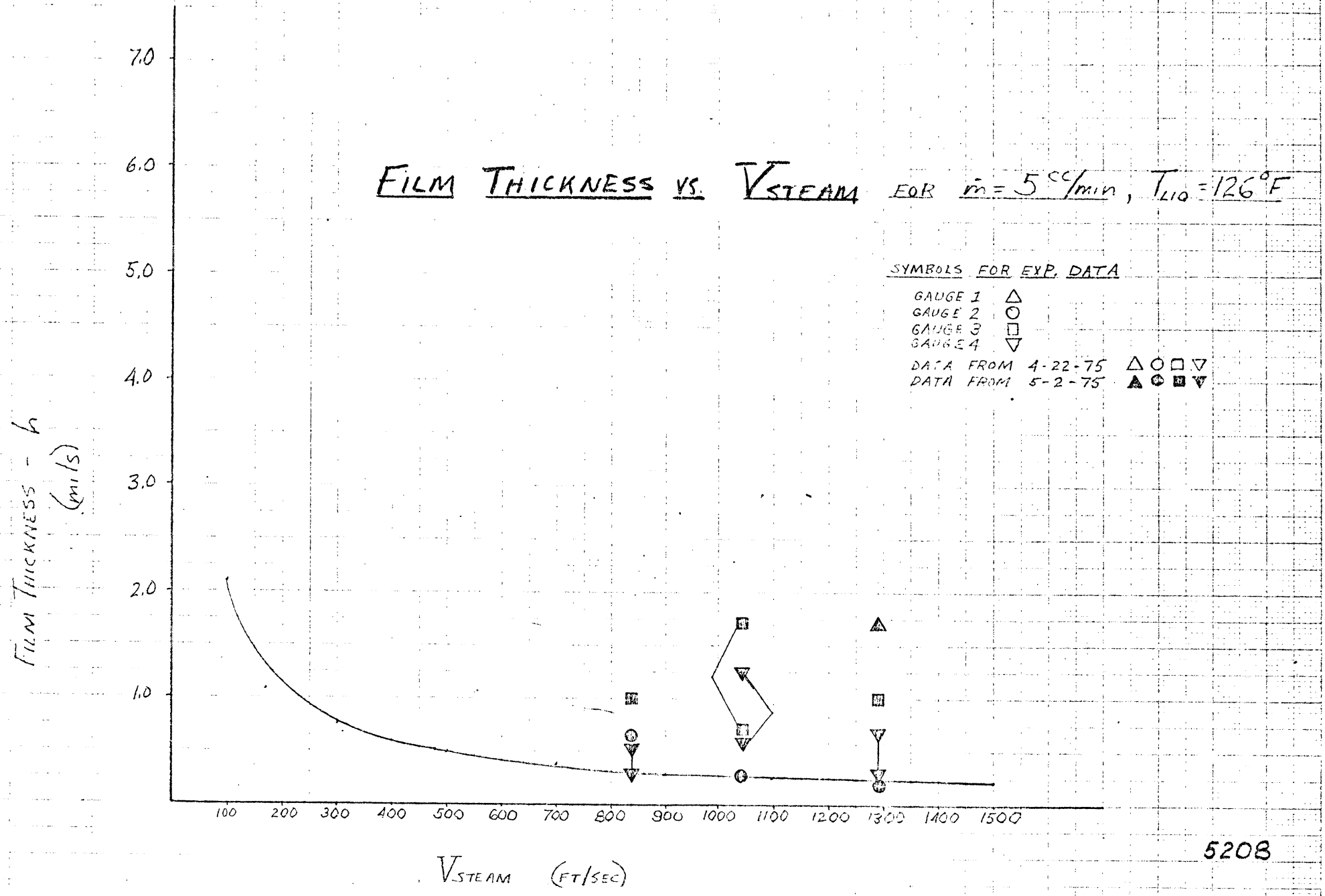

8. Experimental Adiabatic Film Thickness vs Steam Velocity; Liquid Film Flow Rate = 5 cm^3/min.

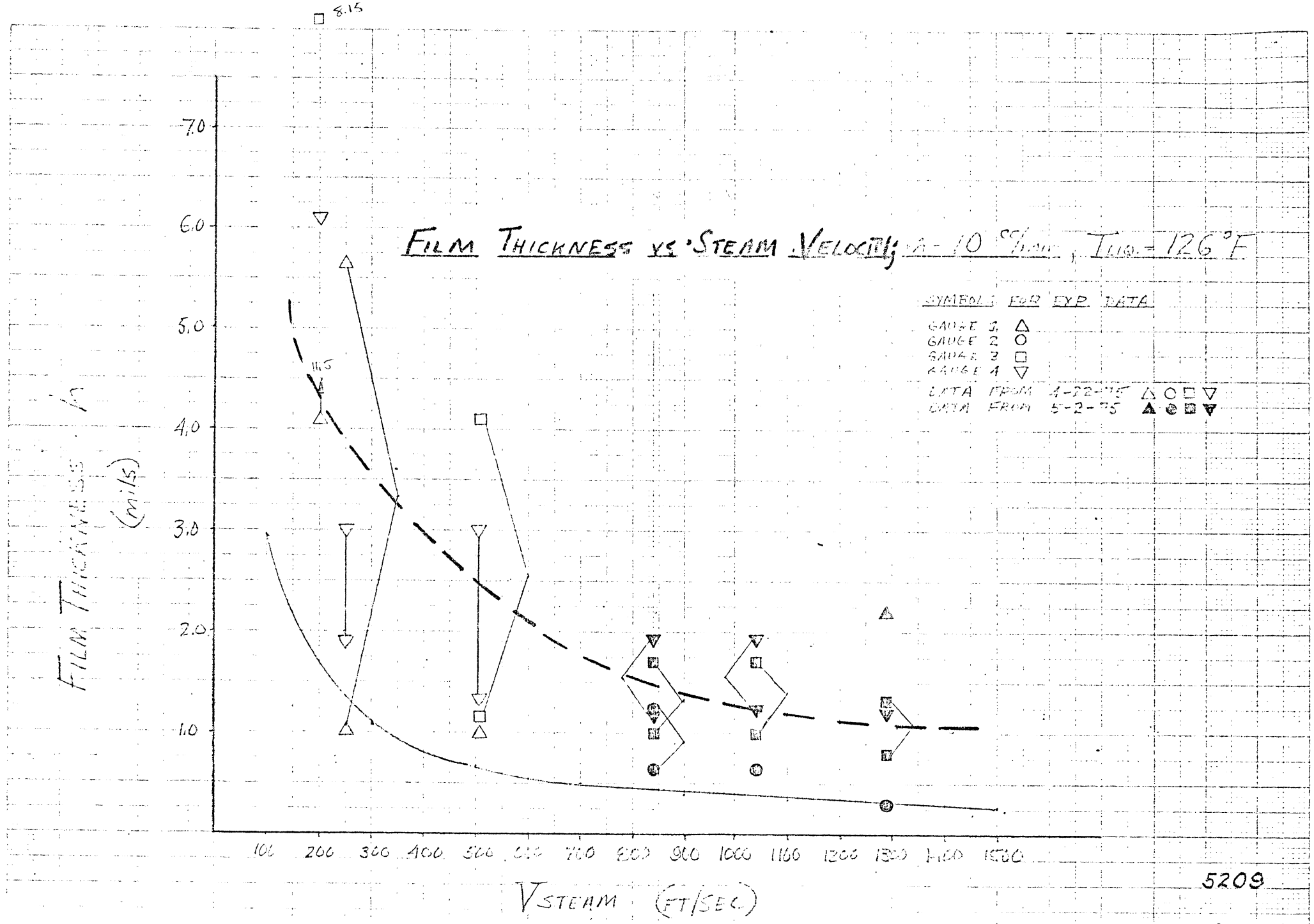

9. Experimental Adiabatic Film Thickness vs Steam Velocity; Liquid Film Flow Rate= 10 cm^3/min.

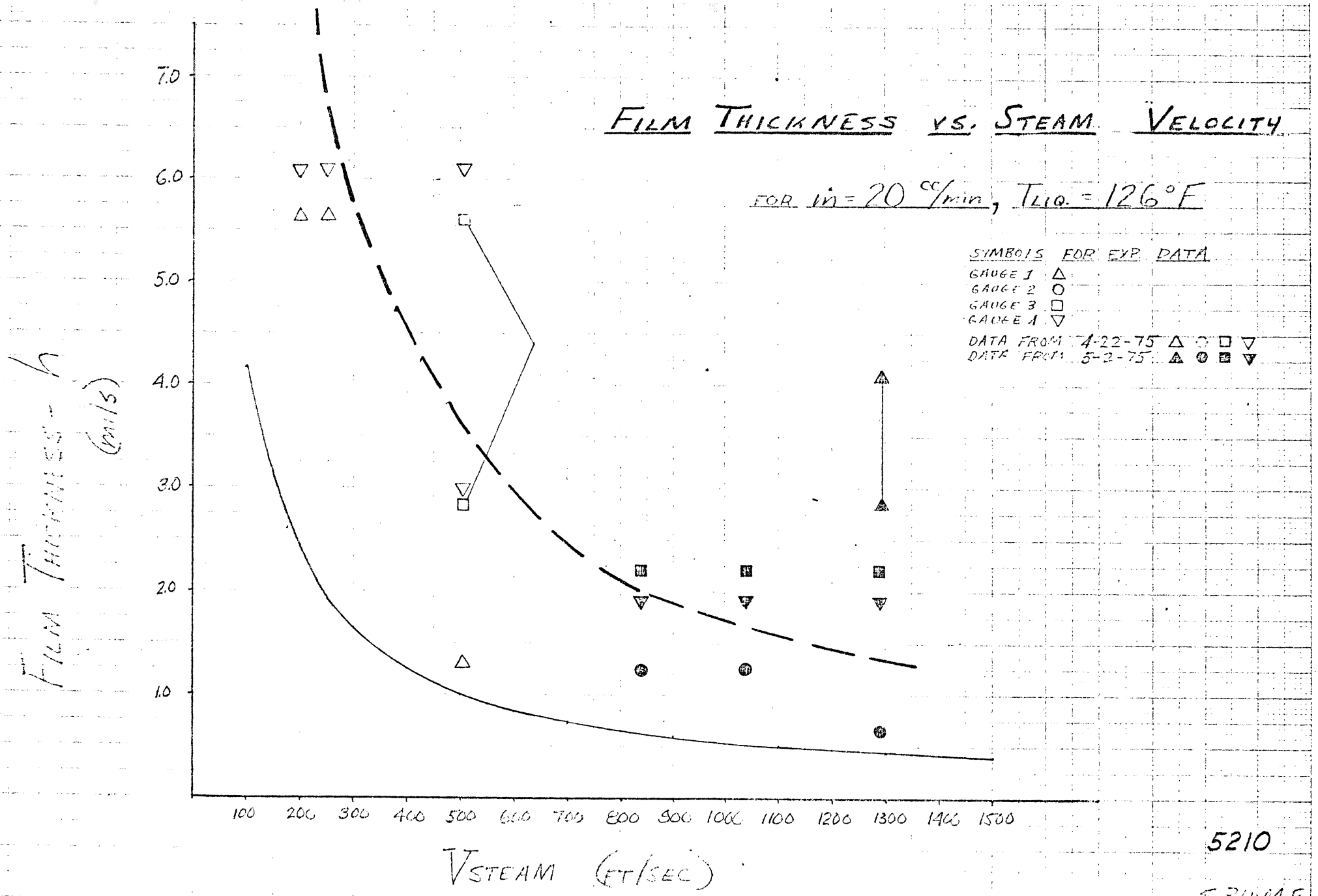

10. Experimental Adiabatic Film Thickness vs Steam Velocity; Liquid Film Flow Rate = 20 cm^3/min.

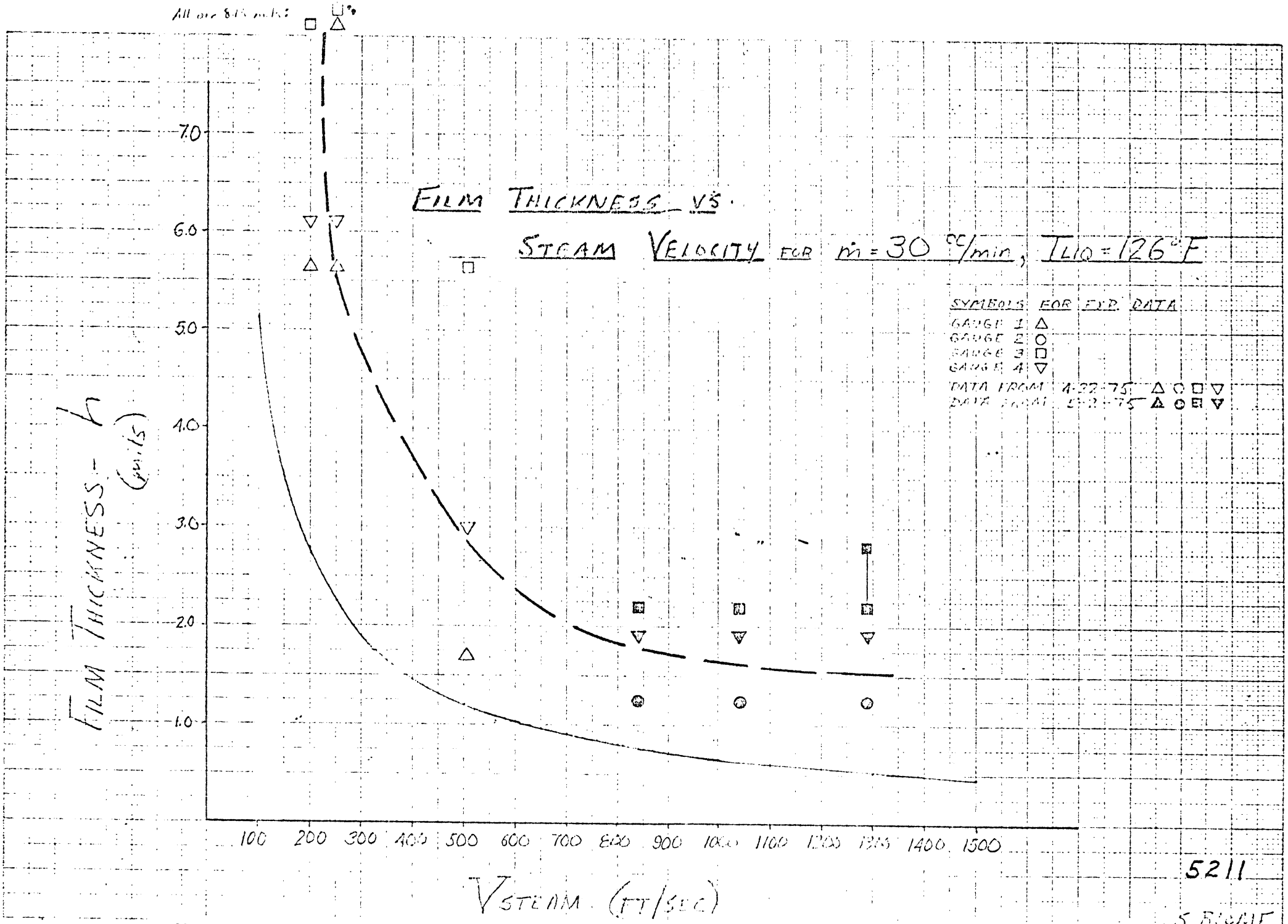

11. Experimental Adiabatic Film Thickness vs Steam Velocity; Liquid Film Flow Rate= 30 cm^3/min

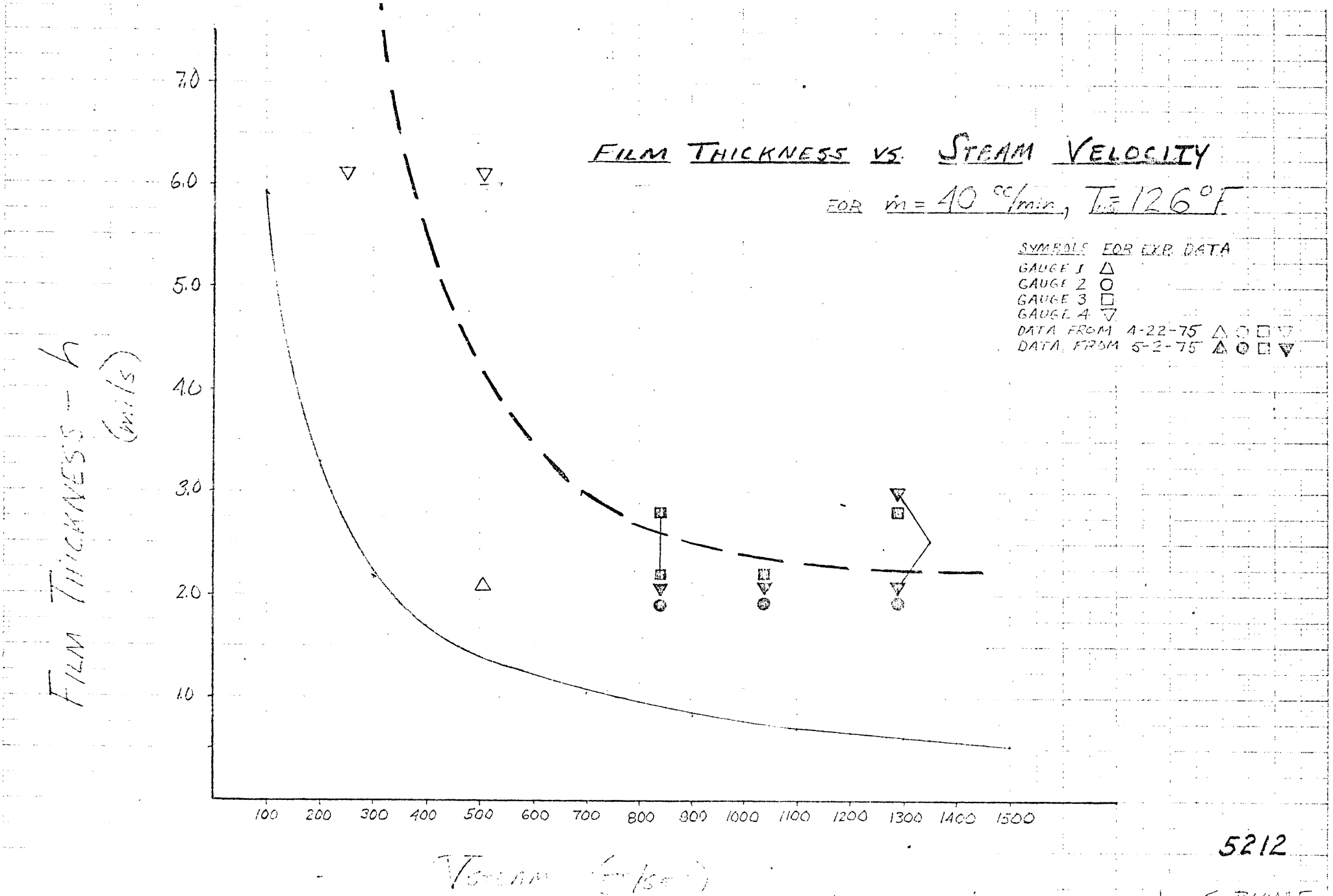

12. Experimental Adiabatic Film Thickness vs Steam Velocity; Liquid Film Flow Rate= 40 cm^3/min.

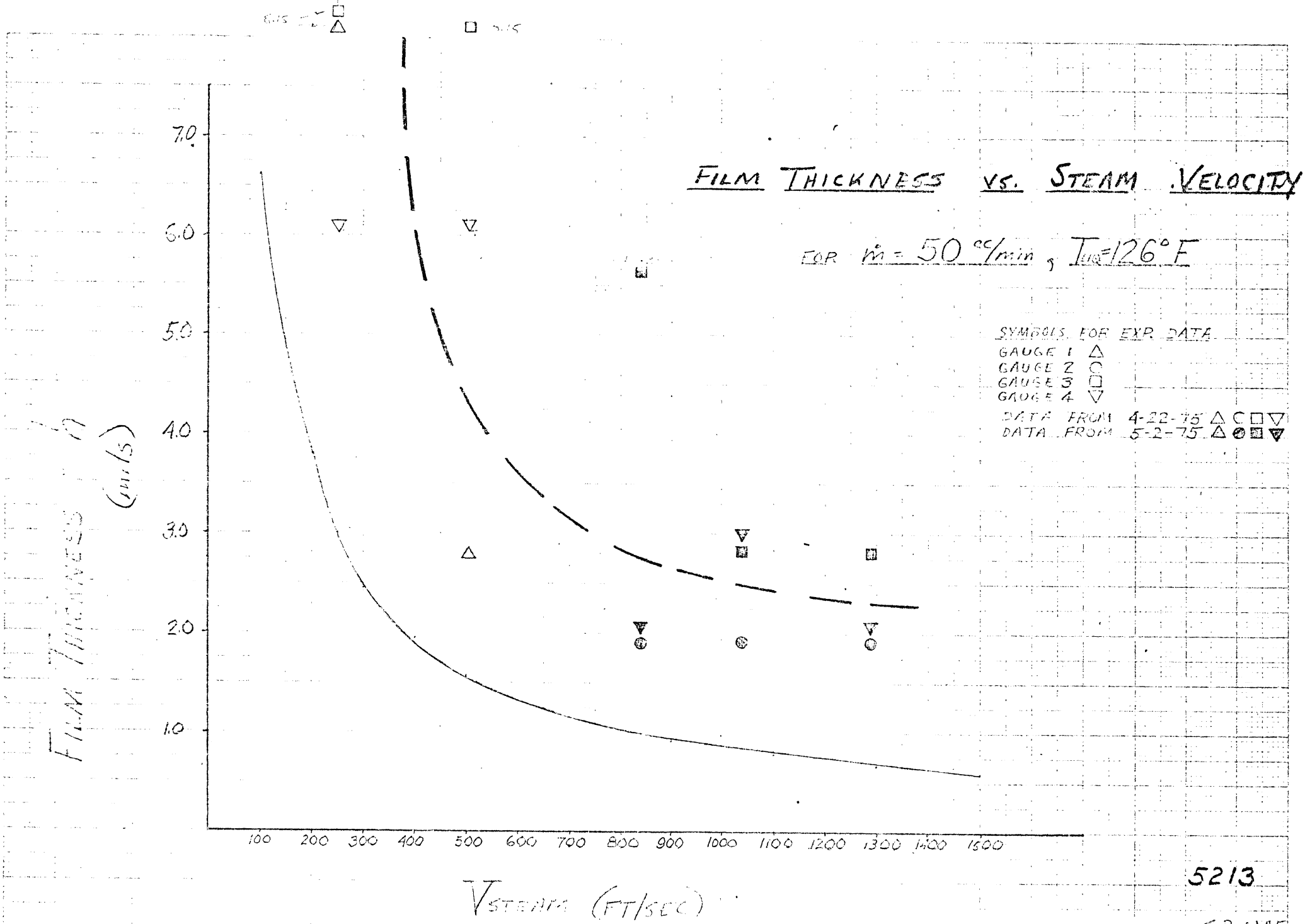

13. Experimental Adiabatic Film Thickness vs Steam Velocity; Liquid Film Flow Rate= 50 cm^3/min.

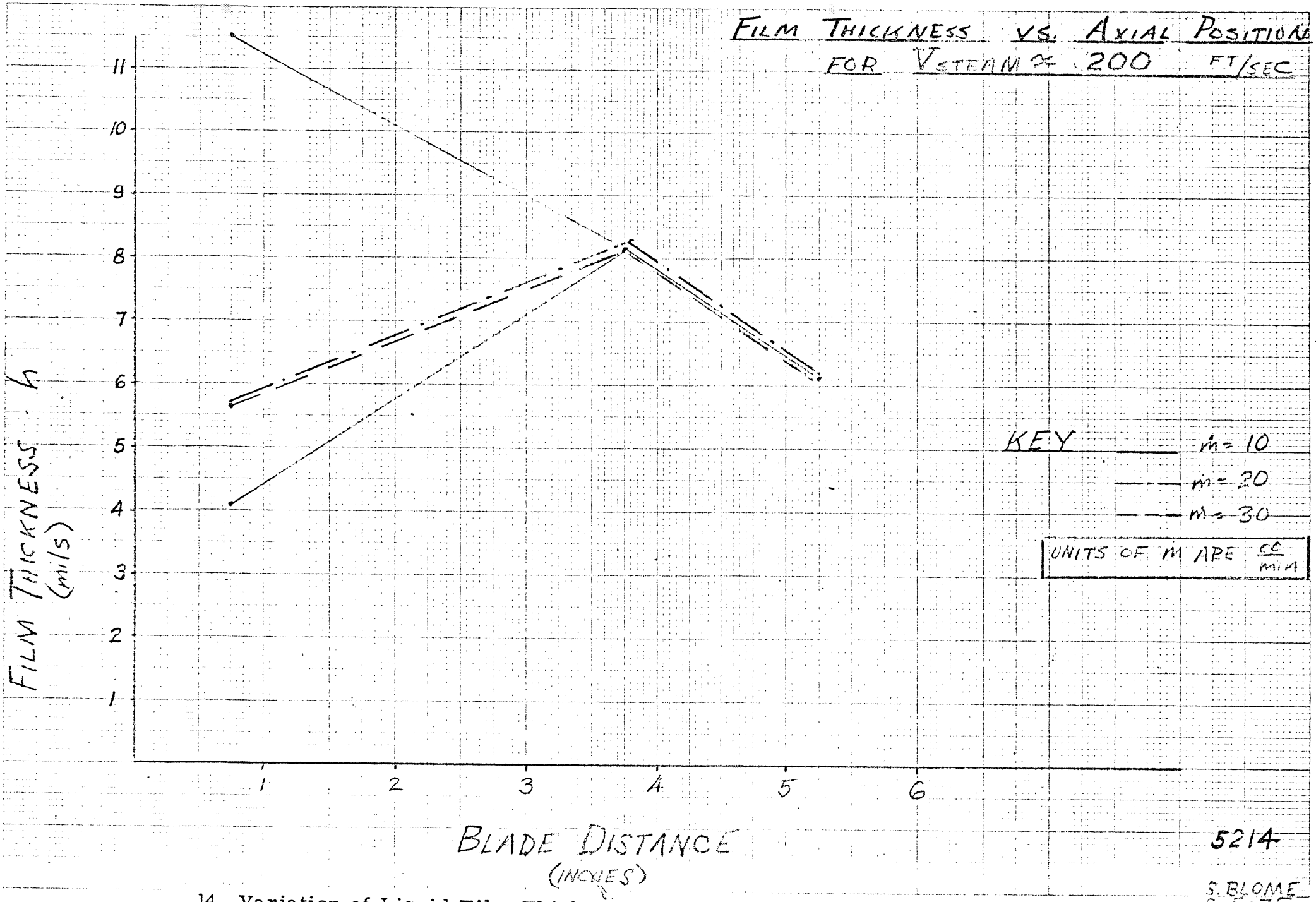

14. Variation of Liquid Film Thickness with Axial Position, Steam Velocity = 200 f/s

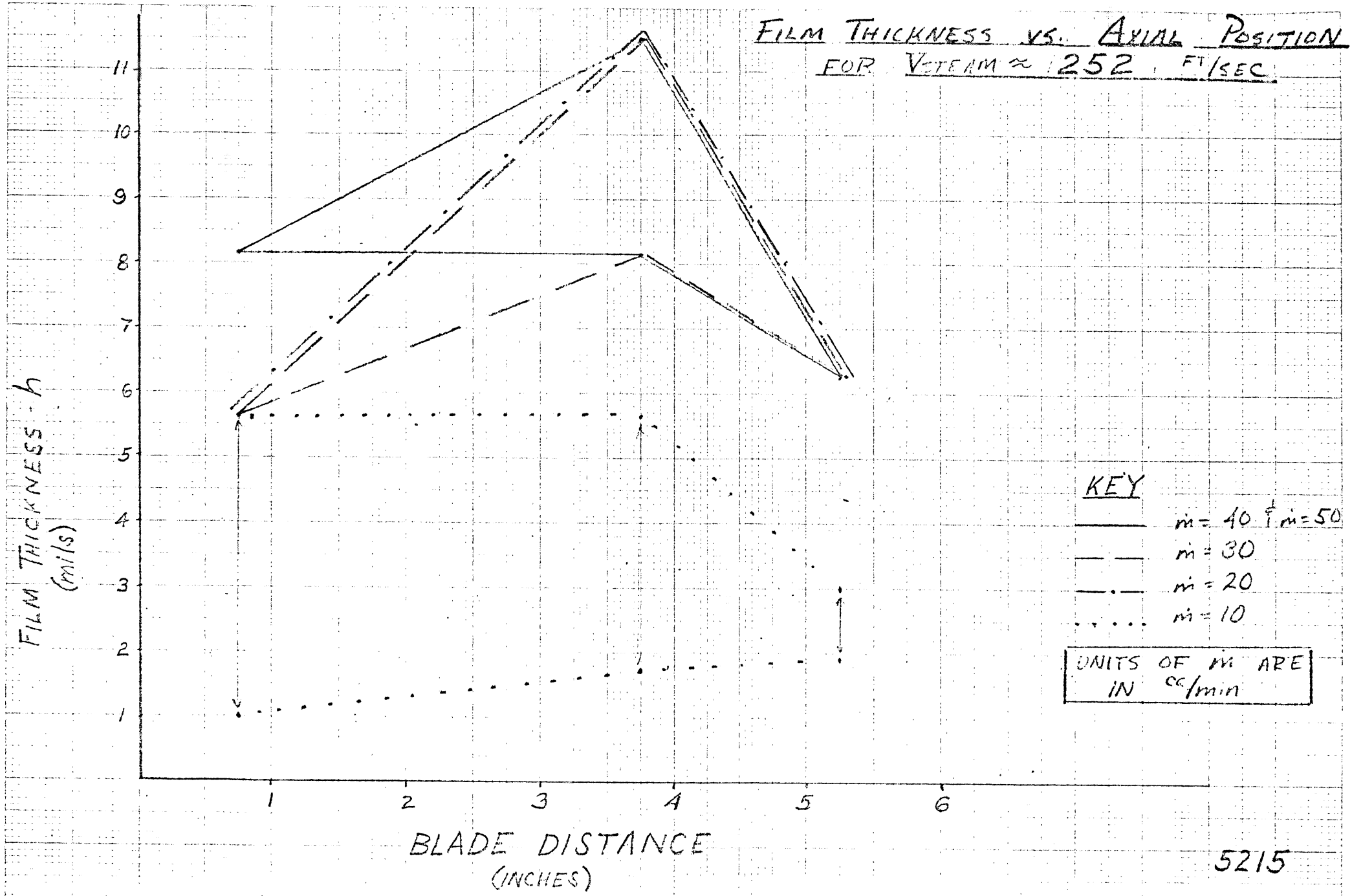

15. Variation of Liquid Film Thickness with Axial Position, Steam Velocity = 252 f/s

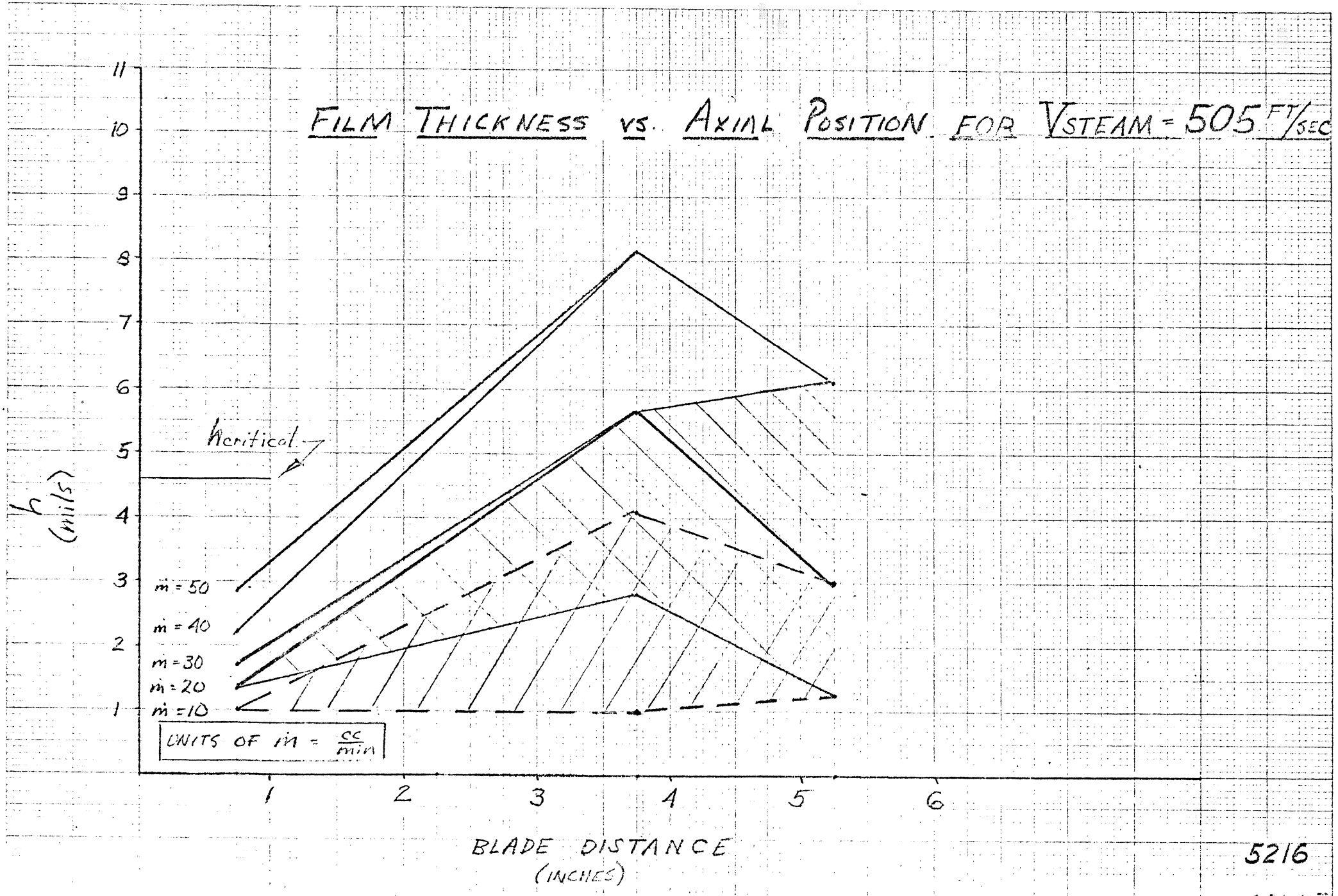

16. Variation of Liquid Film Thickness with Axial Position, Steam Velocity = 505 f/s

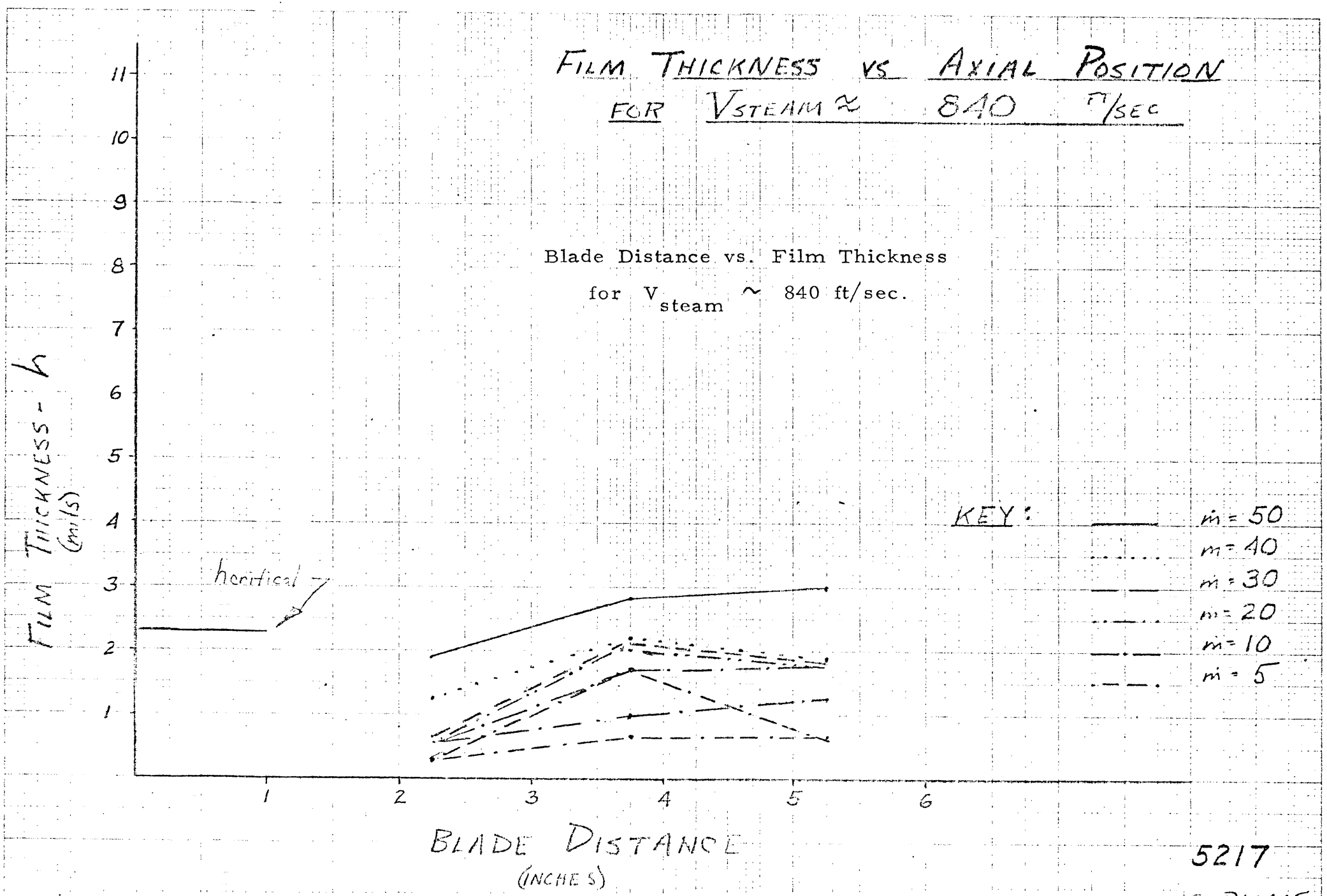

17. Variation of Liquid Film Thickness with Axial Position, Steam Velocity = 840 f/s

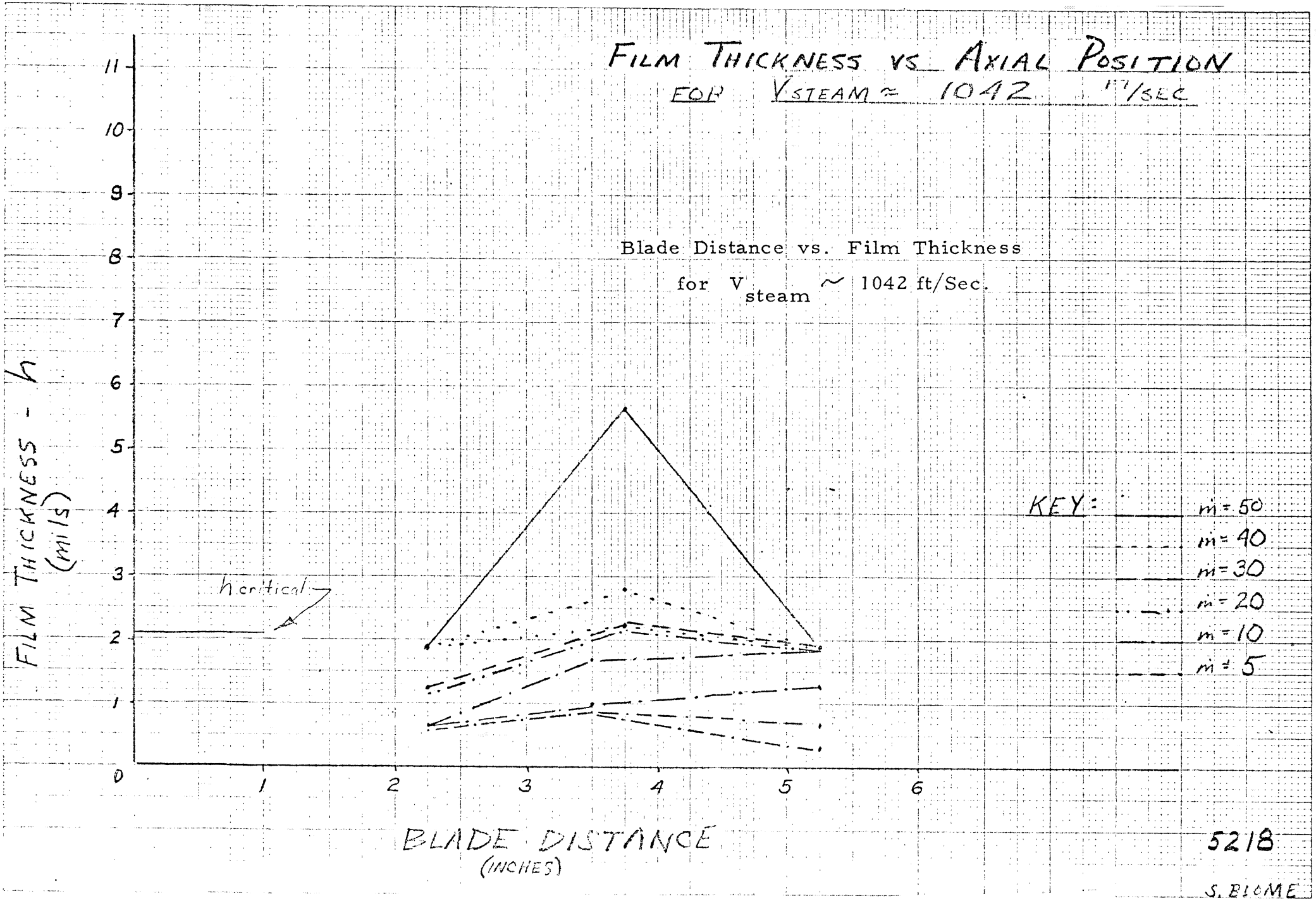

18. Variation of Liquid Film Thickness with Axial Position, Steam Velocity = 1042 f/s

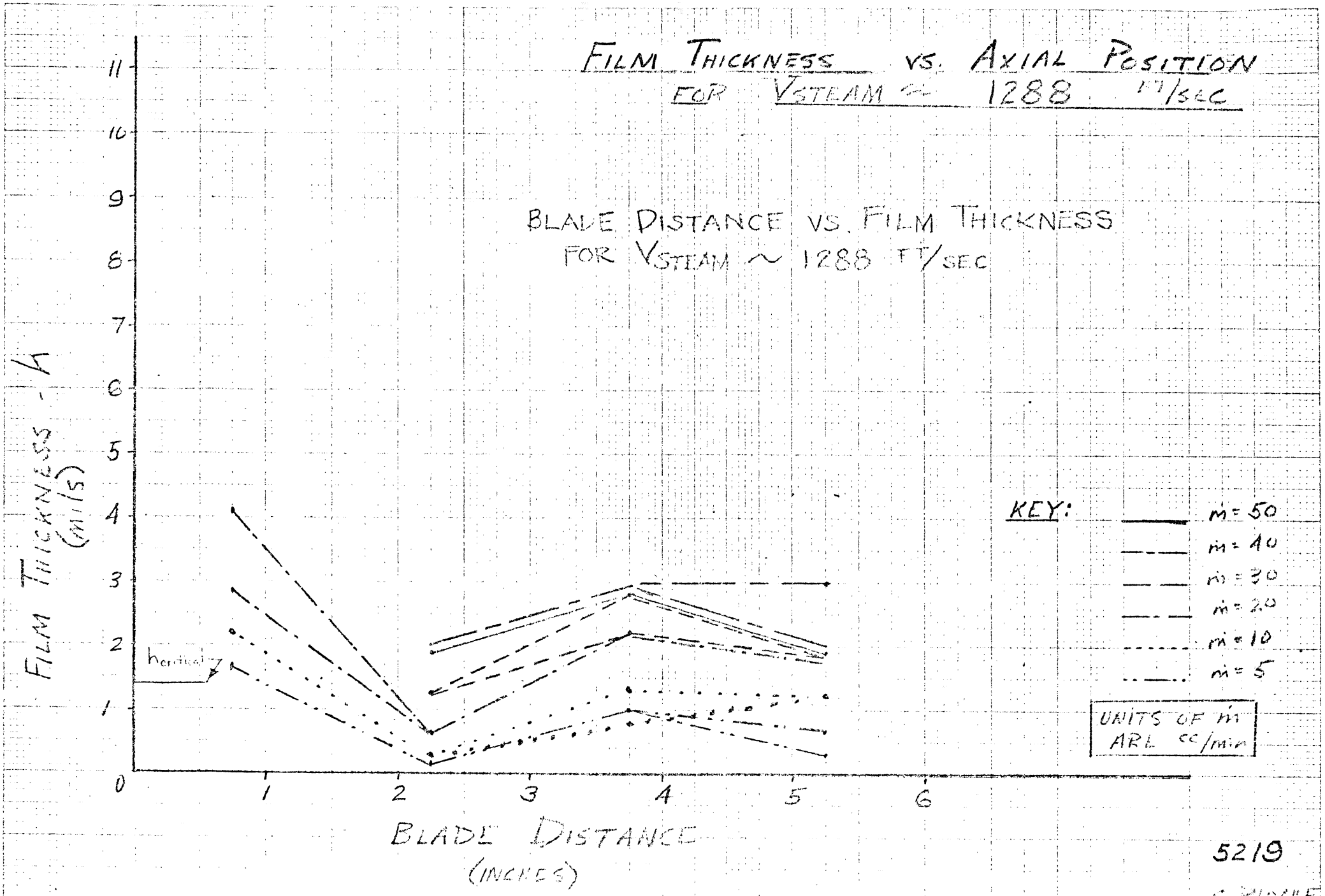

19 Variation of Liquid Film Thickness with Axial Position, Steam Velocity = 1288 f/s

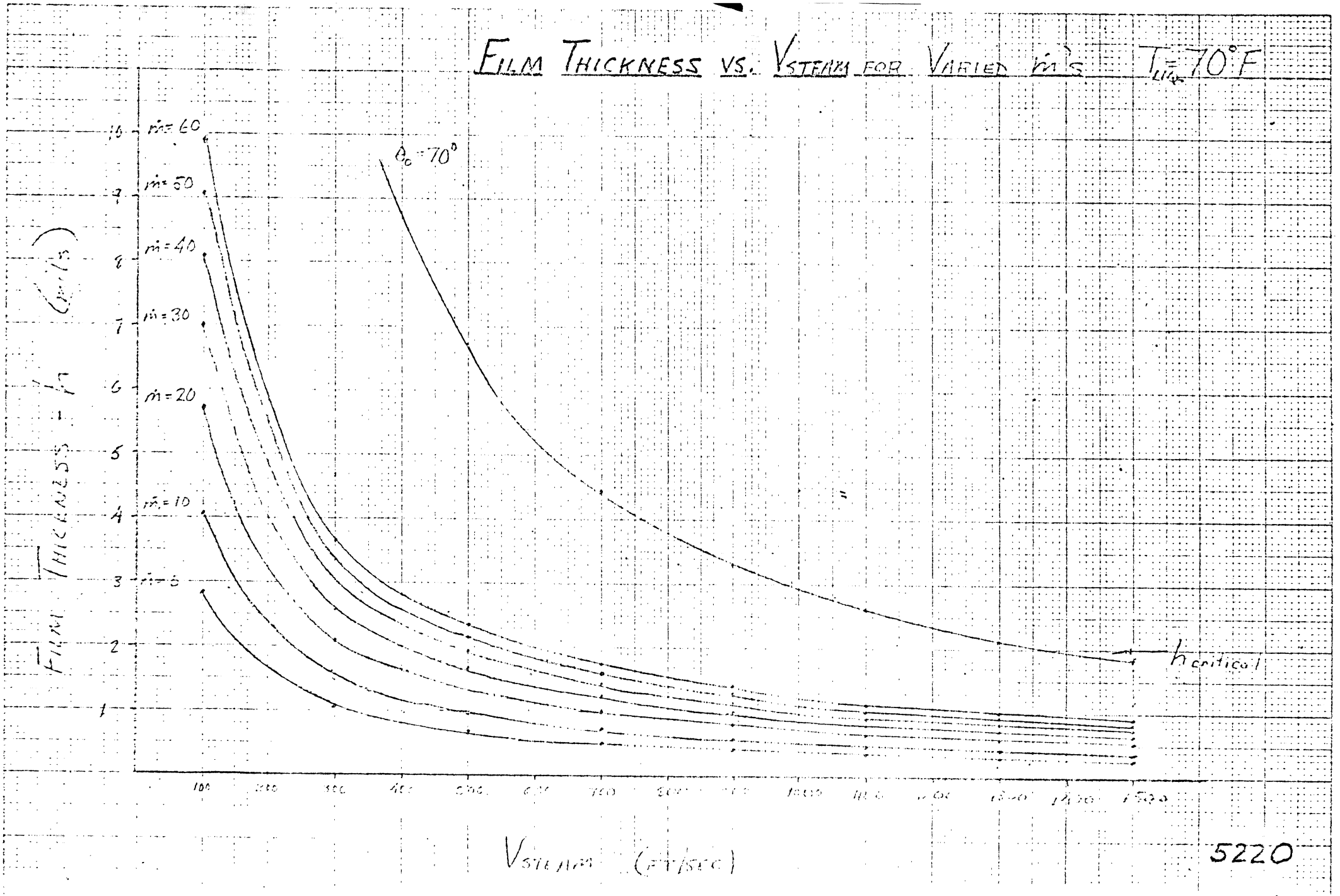

20. Predicted Diabatic (Cold Water) Film Thickness vs Steam Velocity; Various Liquid Film Flow Rates

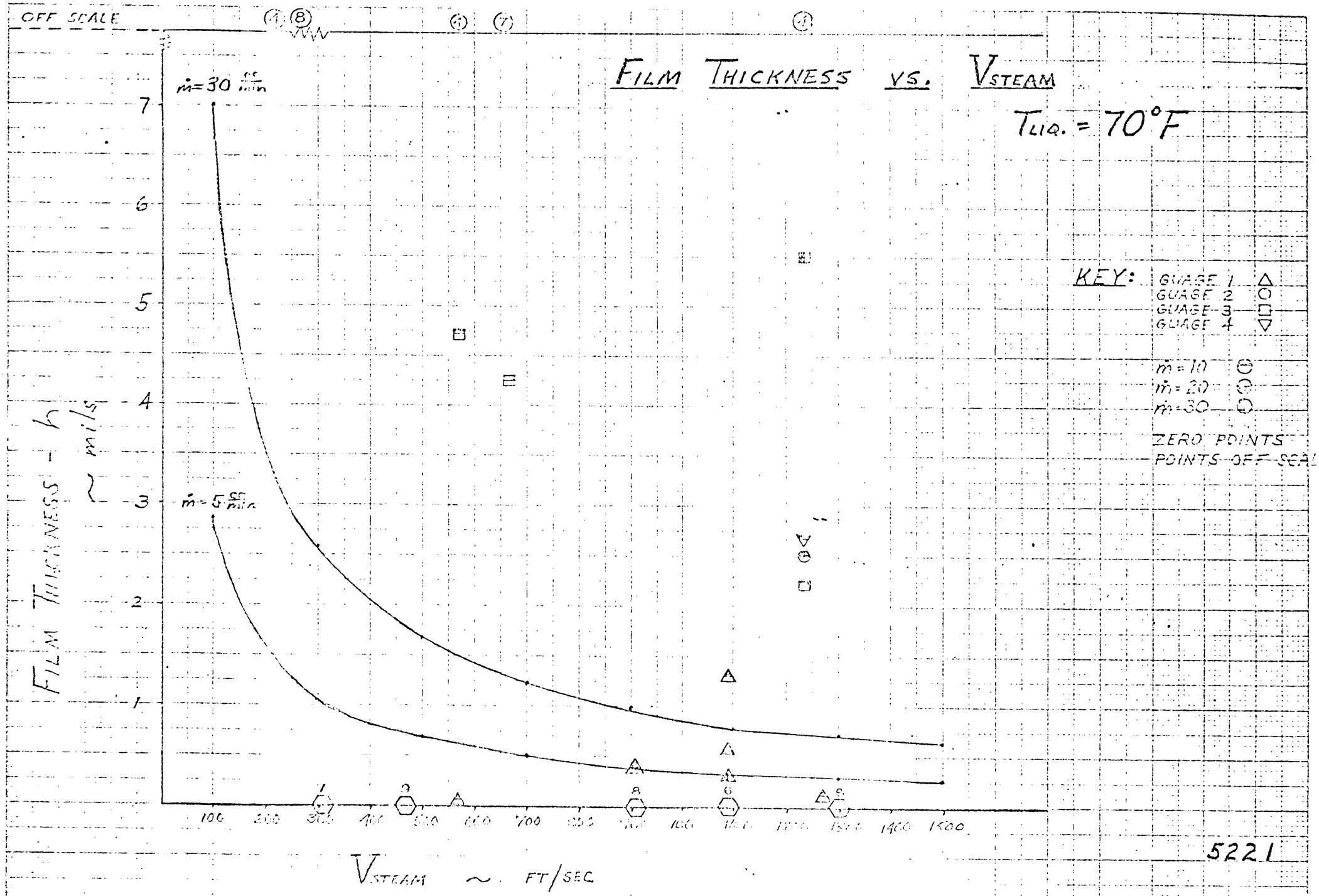

21. Experimental Diabatic (Cold Water) Film Thickness vs Steam Velocity; Various Liquid Film Flow Rates

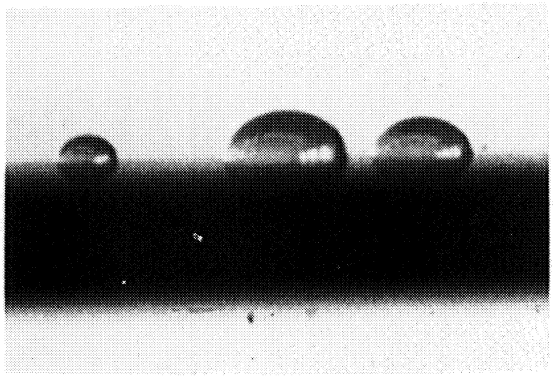

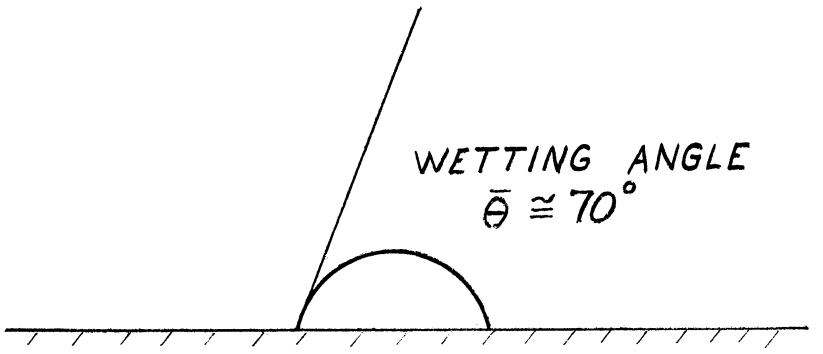

22. Photo of Droplets on Blade #3 Surface Showing Wetting Angle, Θ

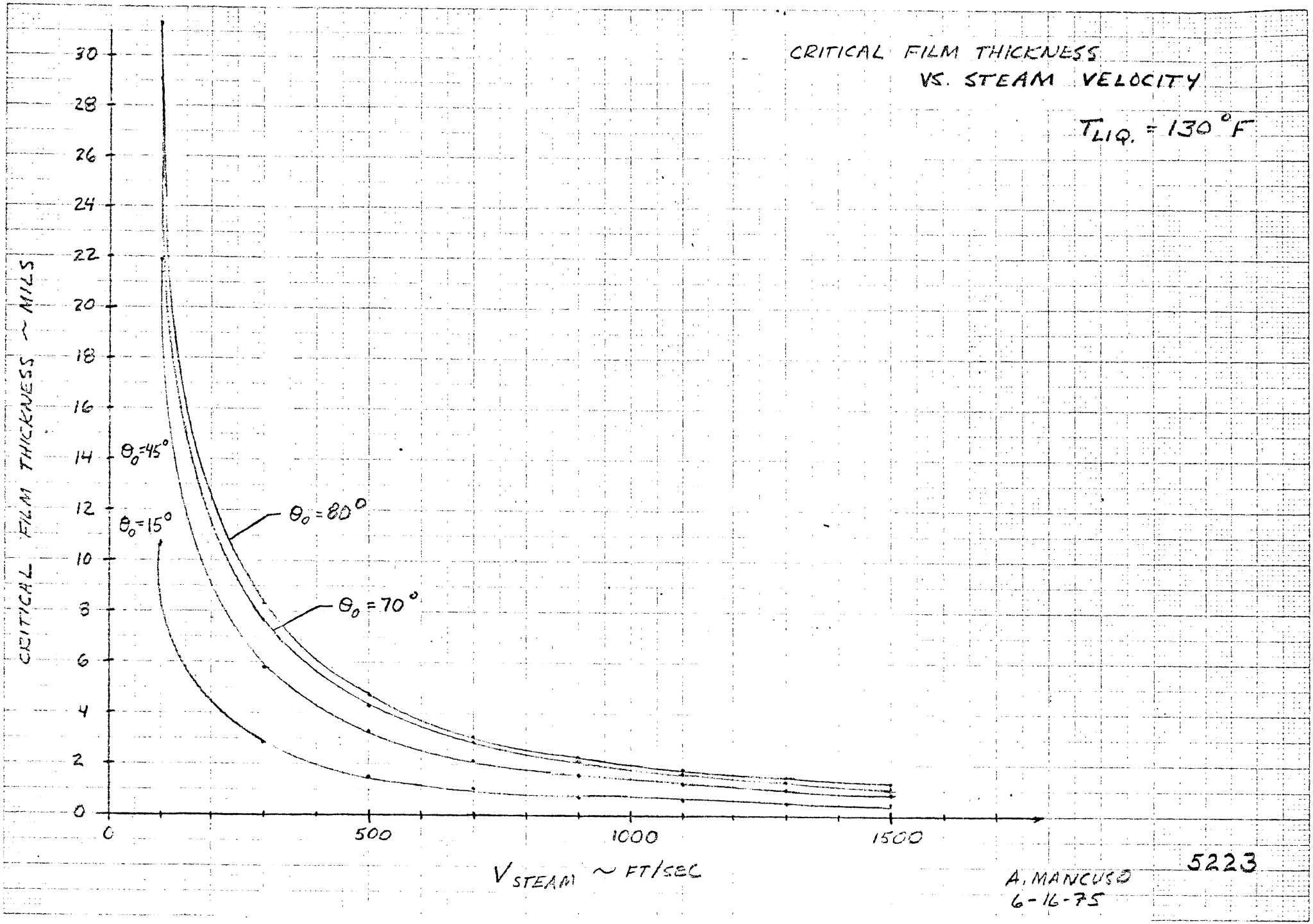

23. Critical Film Thickness vs Steam Velocity, Various Wetting Angles, Liquid Temperature = 130° F (Adiabatic Tests)

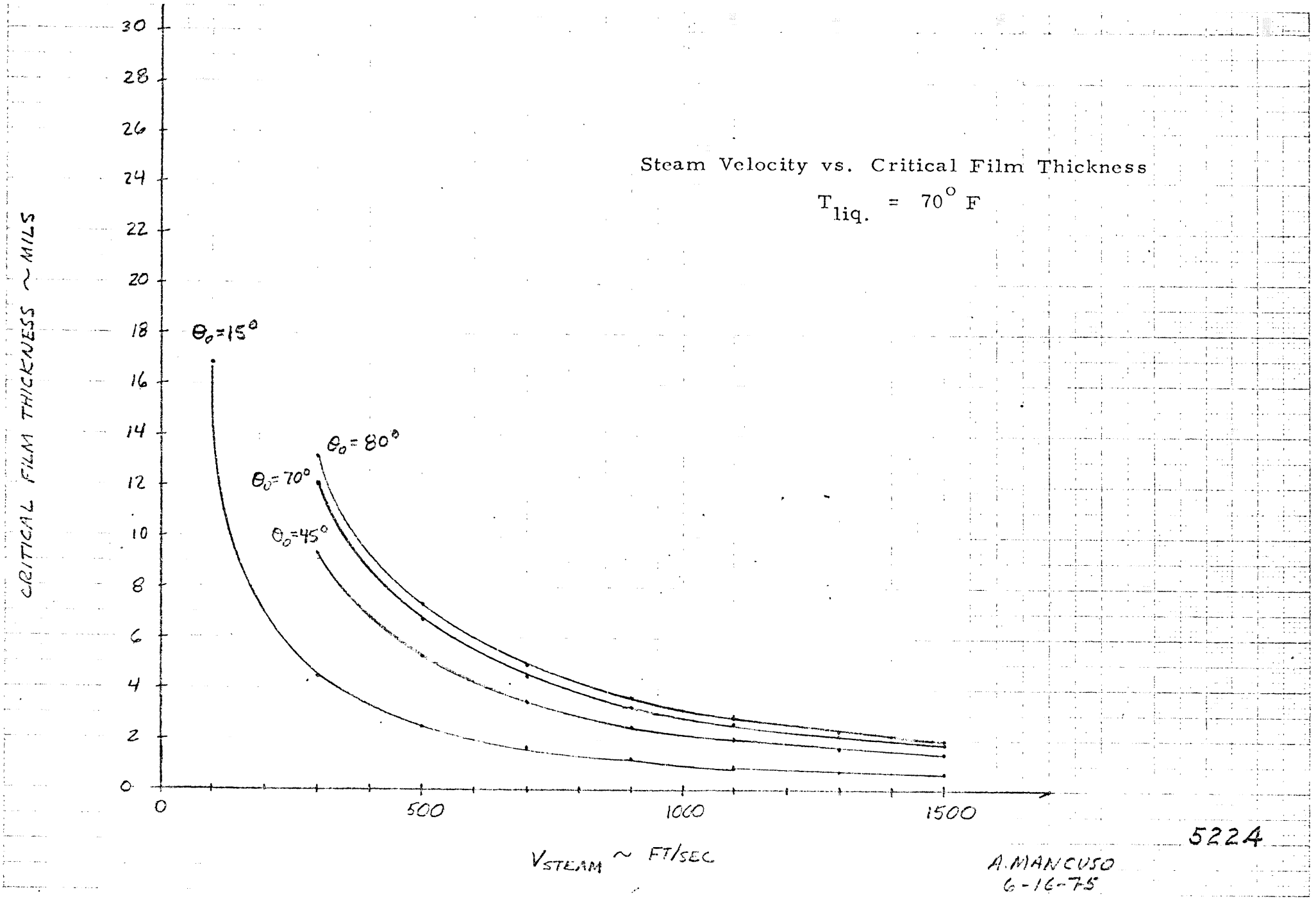

24. Critical Film Thickness vs Steam Velocity, Various Wetting Angles, Liquid Temperature = 70°F (Diabatic Tests)

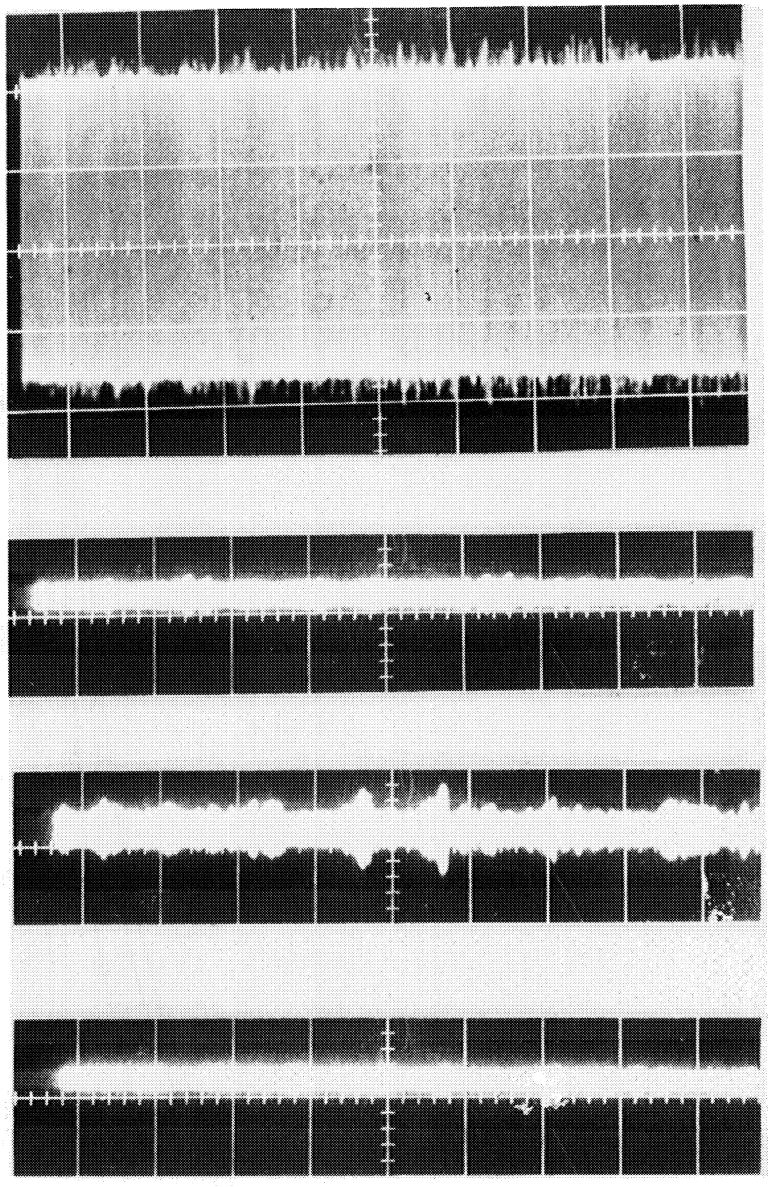

Gauge 1

Gauge 2

Gauge 3

Gauge 4

5225

LIQUID FILM FLOW RATE = 10 cc./min.

SENSITIVITY = 5 volt/cm.

TIME SCALE = 0.5 sec./cm.

DATA FROM 5-29-75

25. Oscilloscope Pictures of Thickness Gage Output

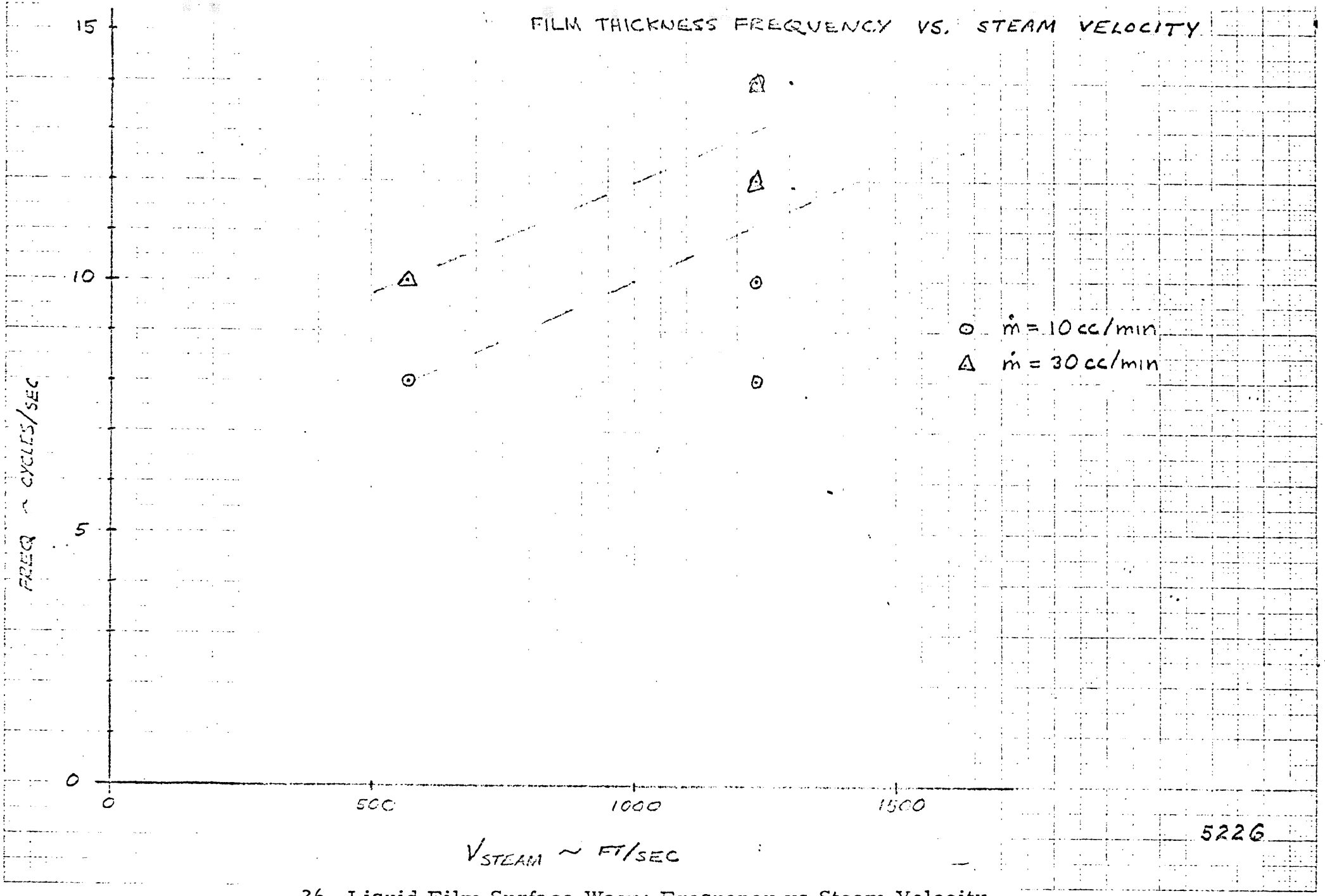

26. Liquid Film Surface Wave; Frequency vs Steam Velocity